Seasonal provenance changes of present-day Saharan dust collected on- and offshore Mauritania

Carmen A. Friese[1], Johannes A. van Hateren[2,*], Christoph Vogt[1,3], Gerhard Fischer[1], Jan-Berend W. Stuut[1,2]

[1]Marum-Center of Marine Environmental Sciences, University of Bremen, Bremen, 28359, Germany

[2]NIOZ-Royal Netherlands Institute for Sea Research, Department of Ocean Systems, and Utrecht University, 1790 AB, Den Burg Texel, Netherlands

[3]ZEKAM, Crystallography, Geosciences, University of Bremen, 28359, Germany

[*]Now at: Vrije Universiteit Amsterdam, Faculty of Earth Sciences, 1081 HV Amsterdam, the Netherlands

Correspondence to: Carmen A. Friese (cfriese@marum.de)

Abstract.

Saharan dust has a crucial influence on the earth climate system and its emission, transport, and deposition are intimately related to e.g. wind speed, precipitation, temperature and vegetation cover. The alteration in the physical and chemical properties of Saharan dust due to environmental changes is often used to reconstruct the climate of the past. However, to better interpret possible climate changes the dust source regions need to be known. By analysing the mineralogical composition of transported or deposited dust, potential dust source areas can be inferred. Summer dust transport offshore Northwest Africa occurs predominantly in the Saharan air layer (SAL). In continental dust source areas dust is also transported in the SAL, however the predominant dust input occurs from nearby dust sources with the low-level trade winds. Hence, the source regions and related mineralogical tracers differ with season and sampling location. To test this, dust collected in traps onshore and in oceanic sediment traps offshore Mauritania during 2013 to 2015 was analysed. Meteorological data, particle-size distributions, back-trajectory and mineralogical analyses were compared to derive the dust provenance and dispersal. For the onshore dust samples, the source regions varied according to the seasonal changes in trade-wind direction. Gibbsite and dolomite indicated a Western Saharan and local source during summer, while chlorite, serpentine and rutile indicated a source in Mauritania and Mali during winter. In contrast, for the samples that were collected offshore, dust sources varied according to the seasonal change in the dust transporting air layer. In summer, dust was transported in the SAL from Mauritania, Mali and Libya as indicated by ferryglaucophane and zeolite. In winter, dust was transported with the Trades from Western Sahara as indicated by e.g. fluellite.

Keywords

Saharan dust, MWAC, sediment trap, mineralogy, particle size, major potential source area, provenance

1. Introduction

Mineral dust influences global climate through many feedback mechanisms and is in turn influenced by variations in environmental parameters. The emission, transport and deposition of mineral dust reacts sensitively to parameters of climate change like rainfall, wind, temperature and vegetation cover (Knippertz and Stuut, 2014). In turn, the emission, transport and deposition of mineral dust has an impact on the atmospheric energy balance (Haywood and Boucher, 2000), precipitation distribution and amplitude (Yoshioka et al., 2007), sea surface temperatures (Lau and Kim, 2007) as well as the oceanic carbon pump (Martin et al., 1991;Martin, 1990;Jickells et al., 2005;Iversen et al., 2010;Iversen and Robert, 2015;Ploug et al., 2008a). The sensitivity of mineral dust to environmental parameters is used to reconstruct the climate of the past (Rea, 1994;Tjallingii et al., 2008;Mulitza et al., 2010;Diester-Haass and Chamley, 1978;Holz et al., 2007;Stein, 1985). For instance, the particle size of mineral dust in ocean sediment records varies according to the paleo-frequency of dust-storm and rainfall events (e.g. Friese et al. (2016)). Further, the mineralogical composition of mineral dust in sediment core records can be used as a qualitative proxy for paleo-dust source activity (Scheuvens et al., 2013).

Every year, about 2000Mt dust are emitted from source areas around the world, of which 75% are deposited on land and 25% into the oceans (Shao et al., 2011).The Saharan Desert is the world's largest source of mineral aerosols with an annual dust transport of ~180 Mt westwards towards the North Atlantic (Yu et al., 2015). About 140Mt is actually deposited into the North Atlantic Ocean (Yu et al., 2015). Therefore, Saharan mineral dust constitutes an essential component of the global climate system. The source regions of Saharan dust have been studied frequently by analysing the mineralogical composition of dust collected at continental sites (e.g. Skonieczny et al. (2013);Skonieczny et al. (2011);Schütz and Sebert (1987);Kandler et al. (2009);Khiri et al. (2004)), during aircraft flights (e.g. Formenti et al. (2008)), on research ships (Chester et al., 1971;Chester et al., 1972;Stuut et al., 2005;Aston et al., 1973;Chester and Johnson, 1971b;Chester and Johnson, 1971a) and with gravity cores offshore NW Africa (Biscaye, 1964;Biscaye, 1965;Lange, 1982;Rateev et al., 1969;Griffin et al., 1968;Diester-Haass and Chamley, 1978;Meyer et al., 2013). Continental dust studies in northern Morocco revealed that dust is produced predominantly locally (Khiri et al., 2004;Kandler et al., 2009). For instance, a high percentage of quartz and feldspar and a low amount of micas in the dust samples was interpreted to represent mostly local dust sources and the availability of calcite sources from proximal coastal dunes in Morocco (Khiri et al., 2004). Further, also in Morocco, dust was sampled in Tinfou at a height of 4 m during the SAMUM 2006 field campaign. These samples were analysed for their physical and chemical properties. The particle size correlated to local surface wind speed suggesting the contribution of local dust (Kandler et al., 2009). In contrast, in coastal Senegal dust is sourced by the Sahel during winter as shown by low illite/kaolinite (I/K) ratios and lower palygorskite contents as opposed to the summer samples which were suggested to be originating from the Sahara (Skonieczny et al., 2013). Further, the I/K ratio in dust sampled on the Cape Verde Islands showed that dust was derived from strongly varying sources: north-western Sahara, central and southern Sahara and the Sahel (Caquineau et al., 2002). The results of the above mentioned studies imply that dust collected on land is predominantly of local provenance, while the sources of dust sampled offshore NW Africa are of regional and long-distance provenance. As a result, a large seasonal difference can be expected in the composition of the marine climate archives, related to the different dominating transport mechanisms of dust in summer and winter (Friese et al., 2016).

To test this, we compared the mineralogical composition, the fluxes, and the particle size of Saharan dust sampled from 2013-2015 in Iwik (Mauritania) in on-land dust traps with Saharan dust sampled from 2013-2015 offshore

Cape Blanc (Mauritania) in sub-marine sediment traps and with the scientific dust-collecting buoy 'Carmen'. By comparing the data with meteorological data, back trajectories, the African lithology and satellite images we aim to address the following questions:

1) What is the seasonal variability in particle size of mineral dust deposited on land? How does the variability relate to meteorological parameters (wind speed, precipitation)?
2) What are the source regions of dust trapped on land versus dust trapped in the ocean?
3) Can we identify characteristic minerals that constitute a tracer for certain source areas?

1.1 Study sites and North African dust sources

In Fig. 1 the location of the study sites and the North African dust sources are displayed. The dust-collecting buoy 'Carmen' (~21°15' N, ~20°56' W) and the sediment trap mooring site CB (~21°16' N, ~20°48' W) are virtually at the same position ~200 nautical miles offshore Cape Blanc. Sediment-trap station CBi (~20°45' N, ~18°42' W) is located ~ 80 nautical miles offshore Cape Blanc. The continental dust collector Iwik (~19°53' N, ~16° 18' W) and the meteorological station Arkeiss (~20° 7' N, ~16° 15' W) are located in a major potential dust source area (**PSA 2**) in the Parc National de Banc d'Arguin (PNBA) near Iwik and near Arkeiss in Mauritania. A further meteorological station is positioned in the **PSA 2** in Nouadhibou (~20° 55' N, ~17° 1' W) in the Western Sahara.

The major PSA of northern African dust are summarized in a review by Scheuvens et al. (2013). Predominant dust transport towards western Africa and offshore the Atlantic Ocean occurs from the foothills of the Atlas mountains, Western Sahara and Western Mauritania (**PSA 2**), southern Algeria and northern Mali (**PSA 3**) and Western Chad including the Bodélé depression (**PSA 5**) (Scheuvens et al., 2013). In contrast, dust sourced from Tunisia and northern Algeria (**PSA 1)** is transported predominantly to the western Mediterranean and Western Europe (Stuut et al., 2009). Central Libya (**PSA 4**) is the most important region for dust transport to the eastern Mediterranean (Scheuvens et al., 2013).

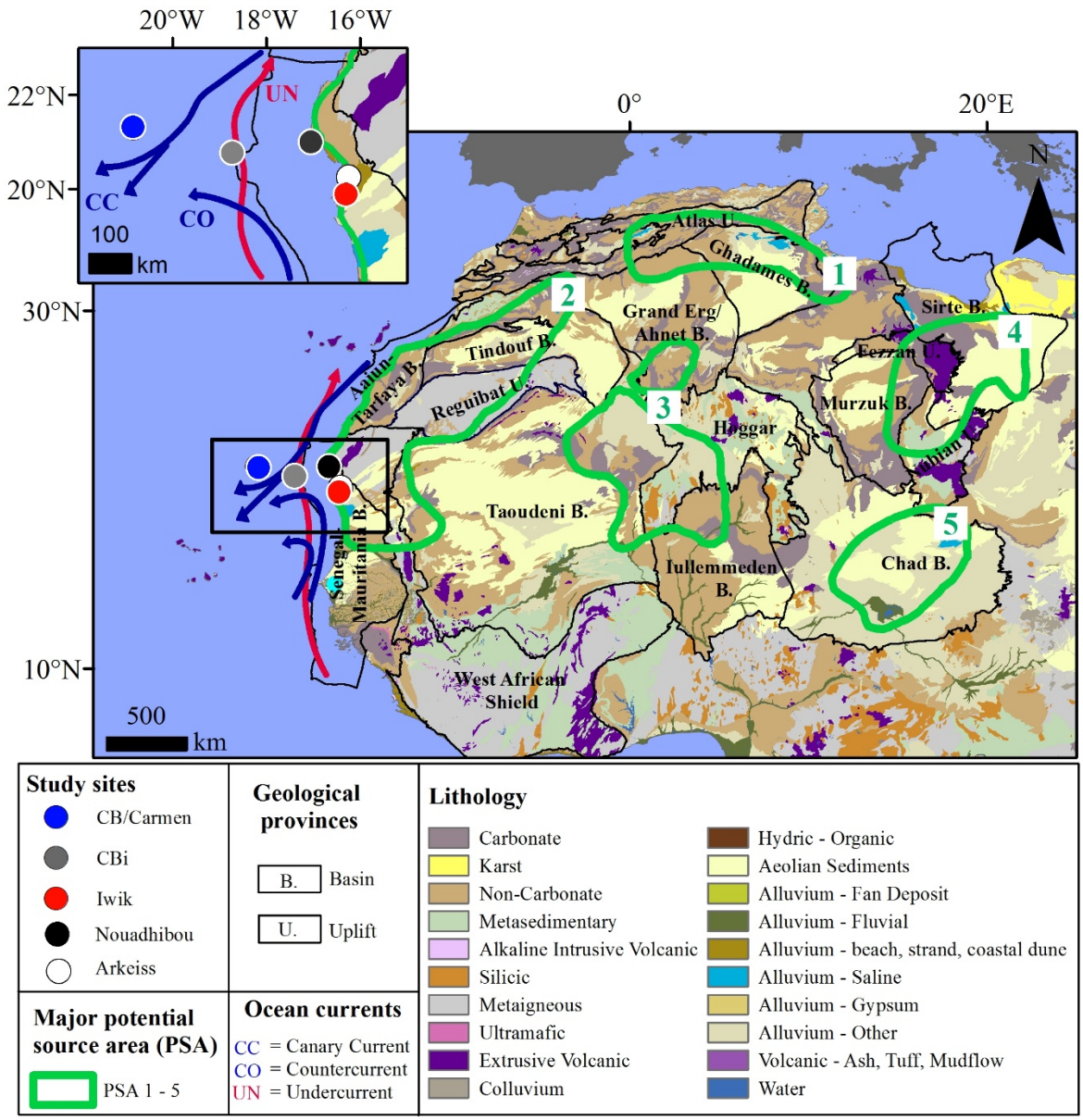

Figure 1: Map of the study sites under investigation: the scientific buoy Carmen as well as the sediment trap moorings CB and CBi offshore Cape Blanc, the MWAC dust collector onshore near Iwik and the surface stations near Nouadhibou and Arkeiss (shapefile of the surface lithology and the geological provinces: downloaded from the USGS website http://rmgsc.cr.usgs.gov/ecosystems/africa.shtml#SL and http://certmapper.cr.usgs.gov/geoportal/catalog/main/home.page, major potential dust source areas: redrawn from Scheuvens et al. (2013), ocean currents: redrawn from Mittelstaedt (1991)).

1.2 Geological characterisation of dust-producing areas

In the following, the lithology of the geological provinces that underlay the major PSA's is outlined (Fig. 1).

The **PSA 1** is underlain by the eastern Atlas chain and the northern Grand erg/Ahnet and Ghadames Basins. The outcrops in the Atlas uplift are composed of e.g. limestones, sandstones and evaporites (Piqué, 2001). The thick strata overlying the northern Ahnet and Ghadames Basin consist of e.g. sandstones and mudstones (Selley, 1997c).

The **PSA 2** is underlain by the Reguibat Shield, the Mauritanides and the Senegal-Mauritania, Aaiun-Tarfaya, Tindouf and Taoudeni Basins. The western part of the Reguibat Shield is dominated by granitic rocks, while the eastern part is dominated by metamorphic and granitic rocks (Schofield et al. (2006) and references therein). West of the Reguibat Shield, the Mauritanides consist of a metamorphic belt and ophiolite (Villeneuve, 2005). West of the Taoudeni Basin, the Mauritanides are characterized by granites, quartzites and strongly metamorphosed rocks (Villeneuve, 2005). While the Aaiun-Tarfaya Basin features outcrops with dolomites and limestones, the Senegal-Mauritania Basin is characterized by very few carbonate deposits (Bosse and Gwosdz, 1996). The Tindouf Basin is characterized by mainly sandy deposits (Selley, 1997a, c). The local soils surrounding the dust collector site Iwik are composed of sandy deposits often rich in fossil shells and partly cemented by lime (Einsele et al., 1974).

The **PSA 3** is underlain by the western Hoggar and parts of the Ahnet, Taoudeni and Iullemeden Basins. The Pharusian belt located in the western Hoggar is characterized by Eburnean granulites, gneiss, graywackes and magmatic rocks (Boullier, 1991). In the southern Ahnet Basin sandstone strata crop out. On the eastern edge of the Taoudeni Basin outcropping sediments are characterized by conglomerates, sandstones and limestones (Bertrand-Sarfati et al., 1991). The outcrops of the Iullemeden Basin are composed of e.g. sandstones, carbonaceous shale, laterites and massive clays (Kogbe, 1973).

The **PSA 4** is underlain by parts of the Fezzan and Nubian uplifts and the Sirte and Murzuk Basins. The eastern Fezzan uplift consists of ocean island basalts (Cvetković et al., 2010;Abdel-Karim et al., 2013), while sediments outcropping in the northern Nubian uplift are composed of e.g. sandstones, limestones and gypsiferous horizons (El Makkrouf, 1988). The southern Sirte Basin is covered by sands, gravel and sand seas (Selley, 1997b). Outcrops of the eastern Murzuk Basin are composed of marine limestones and alluvial sandstones (Selley, 1997c, a).

The **PSA 5** is underlain by the Chad Basin. During the Holocene, the Chad Basin was filled with fine-grained particles from the drainage of the Tibesti mountains to the north (Prospero et al., 2002). Hence, the sediments that outcrop in the central Chad Basin are characterized by fluvial and alluvial sediments such as laminated diatomites, pelites and coastal sandridges (Schuster et al., 2009).

1.3 Atmospheric setting

Saharan dust emission, transport and deposition are related to seasonal variations in atmospheric circulation (Knippertz and Todd, 2012). The intertropical convergence zone (ITCZ) shifts meridionally from ~12 °N during boreal winter to ~ 21 °N during boreal summer resulting in a seasonal change in rainfall and winds over the African continent (Nicholson, 2009).

During summer, continental rainfall is most intense and the rain belt is positioned near ~10°N with smaller amounts of rainfall near ~ 21°N. Dust emission is driven by low level jets, 'haboobs', African easterly waves (AEWs) and high surface winds associated with the Saharan heat low (Knippertz and Todd, 2012). Low-level N trade winds blow and transport dust in coastal Mauritania year-round (National Geospatial-Intelligence Agency, 2006). Saharan dust is transported on- and offshore within the 'Saharan air layer' (SAL) at an altitude of about 3 km (Diaz et al., 1976;Carlson and Prospero, 1972;Prospero and Carlson, 1972;Prospero and Carlson, 1970).

During winter, dust emission is driven by the break-down of nocturnal low-level jets after sunrise, increased surges in Harmattan winds and microscale dust devils and dust plumes (Knippertz and Todd, 2012;Koch and Renno, 2005). Dust is transported within the NE and E trade winds to coastal Mauritania (Dobson, 1781) and also offshore to the sediment-trap mooring sites (Stuut et al., 2005).

1.4 Oceanic setting

The surface-water circulation offshore Cape Blanc is influenced by the southward-flowing Canary Current (CC) and the poleward-flowing coastal counter current or Mauritania Current (Fig. 1). Underneath, the undercurrent is flowing poleward in water depths down to 1000 m (Fig. 1). The undercurrent flows along the continental slope and transports water masses originating from ~5-10 °N to latitudes up to 26 °N. The poleward flowing South Atlantic Central Water (SACW) and the southward flowing North Atlantic Central Water (NACW) are situated below the counter current and meet offshore Cape Blanc (Mittelstaedt, 1991). The study area is positioned in a zone of permanent annual upwelling of sub-surface water masses (Cropper et al., 2014). The NACW and SACW may be upwelled and mixed laterally off Cape Blanc (Meunier et al., 2012). The permanent annual upwelling of nutrient-rich subsurface waters results in high phytoplankton concentrations offshore Cape Blanc (Van Camp et al., 1991). As a result, the surface waters are rich in organic detritus, usually referred to as ‘marine snow’, and faecal pellets which are produced by marine zooplankton (Iversen et al., 2010).

Individual Saharan dust particles which settle at the ocean surface hardly settle to the deep sea. Instead, fine dust particles can be transferred from the ocean surface to the deep sea by being incorporated into marine snow aggregates and faecal pellets (Ternon et al., 2010). The aggregate formation and ballasting of marine snow aggregates and faecal pellets with marine carbonate and opal as well as with Saharan dust particles results in anomalously high sinking velocities (Iversen and Robert, 2015;Fischer and Karakas, 2009;Iversen and Ploug, 2010;Iversen et al., 2010;Ploug et al., 2008b). Dust-loaded particles that sink into the deeper water column are assumed to have a mean settling speed of ~ 240 m d^{-1} at site CB (Fischer and Karakas, 2009).

2. Material and Methods

In Table 1 an overview of the material and methods employed for each study site is presented. Bulk sediment samples were obtained at the sites CB and CBi and dust samples at the sites Carmen and Iwik. All samples were analyzed for particle size and dust flux with the exception of the site Carmen, of which only dust particle size was analyzed. Only the sites CBi and Iwik were analyzed for mineral assemblages and only the samples of the site Iwik were used for microscopic investigation. Meteorological sensors were available for the stations Carmen, Iwik and Arkeiss, while for the site Nouadhibou meteorological data was downloaded online. TRMM precipitation data was downloaded online for all sites except for the site Nouadhibou.

Table 1: Overview of the material and methods employed at each study site.

Study site	Lat./Lon.	Samples	Analysis	Meteorological sensor and data	Downloaded meteorological data
Carmen	~21°15' N, ~20°56' W	1 MWAC sample	particle size	Vaisala WXT520: wind direction + speed, precipitation	TRMM 3B42: precipitation
CB	~21°16' N, ~20°48' W	38 sediment trap samples	lithogenic fluxes, particle size	-	TRMM 3B42: precipitation
CBi	~20°45' N, ~18°42' W	38 sediment trap samples	lithogenic fluxes, particle size, mineral assemblages	-	TRMM 3B42: precipitation, HYSPLIT back trajectories
Iwik	~19°53' N, ~16° 18' W	24 MWAC samples	microscopy, dust fluxes, particle size, mineral assemblages	Davis 6250 Vantage Vue: wind direction + speed	TRMM 3B42: precipitation, HYSPLIT back trajectories
Nouadhibou	20° 55' N, 17° 1' W	-	-	-	Wind direction + speed
Arkeiss	~20° 7' N, ~16° 15' W	-	-	Davis 6250 Vantage Vue: precipitation	TRMM 3B42: precipitation

2.1 Sediment traps

Saharan dust was collected in the ocean using marine sediment traps of the type Kiel (model SMT-234/243) which are conical with an opening of 0.5 m^2 (Fig. 2). The principle of particle collection is much the same as described by Van der Does et al. (2016b) and Korte et al. (2017). At the top of the opening a honeycomb grid is installed to prevent large swimmers (>1 cm) from entering the trap. The sediment traps were equipped with twenty sample cups which rotated according to a pre-programmed sampling interval (Fischer and Wefer, 1991). The sampling interval was chosen depending on the timing of the ship expeditions.

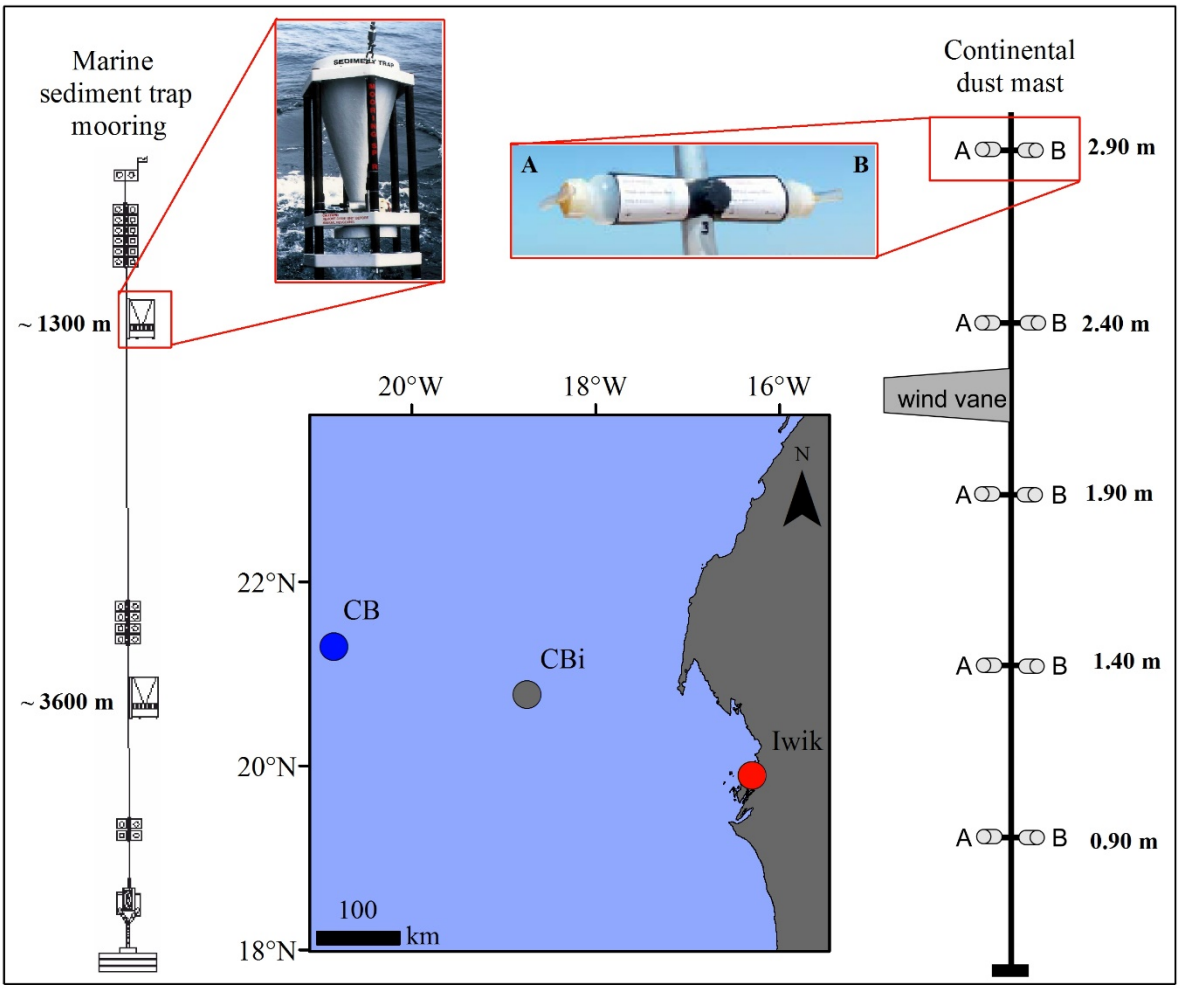

Figure 2: The marine sediment trap moorings CB and CBi offshore Cape Blanc and the dust masts near Iwik, Mauritania. On the left, a sketch of the sediment trap mooring (sketch of CB 24 copied from Fischer et al. (2013)) together with a photograph of the trap (downloaded from www.kum-kiel.de) is displayed. On the right, a sketch of the dust mast together with a photograph of the MWAC sampling bottles is depicted.

The sampling intervals were synchronized between the two sites. The intervals ranged from 9.5 days to 21.5 days (Table 2). Deployment and recovery of the sediment-trap samples was performed during the Research Vessel Poseidon expeditions POS445 (Fischer et al., 2013), POS464 (Fischer et al., 2014) and POS481 (Fischer et al., 2015) (Table 2). The working steps related to the trap deployment and treatment are described in Fischer and Wefer (1991). In order to prevent outflow of water from the cups during sampling, each sampling cup was filled with 20 ml of filtered (<0.2 µm) seawater with a salinity of 40 ‰. To produce seawater with a salinity of 40 ‰, 100 g NaCl suprapur was added to 1 l of filtered seawater. Microbial and zooplankton activity was inhibited inside the trap samples by adding 1 ml of a saturated solution of the biocide $HgCl_2$ per 100 ml of seawater. After recovery, swimmers <1 cm were removed from the samples by sieving each sample through a 1 mm mesh. A McLane rotary liquid splitter was used to split the <1 mm fraction of each sample into five equal aliquots.

The samples of two sediment-trap deployments during 2013-2015 of the sediment trap mooring stations CB and CBi were chosen for grain-size analyses (Table 2). The upper traps sampled at an average water depth of ~ 1300 m and the lower trap sampled at a water depth of ~3600 m (Table 2). Dust which settles at the ocean surface is advected by ocean currents during settling in the water column. As a result, particles that settle in an area of ~ 40

x 40 km^2 in the ocean surface above the traps may be collected in a water depth of ~ 1300 m (Friese et al., 2016). Two winter and two summer samples were chosen for X-ray Diffraction (XRD) measurements (Table 3).

Table 2: Specifications of the sediment trap samples collected during 2013-2015 chosen for flux and grain-size analysis.

Trap series	Trap type	Sampling period	Cruise deployment	Cruise recovery	Position	Trap depth [m]	Water depth [m]	No. of samples	Sampling intervals
CBi 11 upper (GeoB 18006-2)	SMT 243	29.01.2013 – 25.03.2014	Pos445	Pos464	20°46.4' N 18°44.4' W	1406	2800	18	17x21d, 1 x20d
CBi 12 upper (GeoB 19402-01)	SMT 234 NE	14.02.2014 - 23.02.2015	Pos464	Pos481	20°46.4' N 18°44.5' W	1356	2750	20	1x12.5 d, 19x19.5
CB 24 upper (GeoB 18001-1)	SMT 234 NE	24.01.2013 - 05.02.2014	Pos445	Pos464	21°16.9' N 20°50.6' W	1214	4160	18	1x26 d, 16x21 d, 1x15 d
CB 25 lower (GeoB 19401-1)	SMT 234 NE	07.02.2014 – 21.02.2015	Pos464	Pos481	21°17.8' N 20°47.8' W	3622	4160	20	19x19.5 d, 1x9.5 d

Table 3: Sediment trap and MWAC samples chosen for mineralogical investigation.

Sample	Sampling period	Mast	Bottle	Elevation/water depth [m]	Sampling interval
CBi 11 upper # 8	25.06.-16.07.13	-	-	1406	21d
CBi 12 upper # 2	26.02.-18.03.14	-	-	1356	20d
CBi 12 upper # 10	01.08.-21.08.14	-	-	1356	20d
CBi 12 upper # 17	16.12.-04.01.15	-	-	1356	19d
Iwik 13-7-2-3B	24.06.-15.07.13	2	B	1.90	21d
Iwik 14-8-2-5B	15.08.-15.09.14	2	B	2.90	31d
Iwik 14-12-1-4A	15.12.14-18.01.15	1	A	2.40	34d
Iwik 14-2-2-5B	15.02.-15.03.14	2	B	2.90	28d

2.2 Modified Wilson and Cooke (MWAC) samplers

Saharan dust was collected on land near Iwik, Mauritania, with a passive dust sampler consisting of two masts (1 and 2) with two sets of five air sampling bottles each (A and B, Fig. 2). The dust sampling bottles are referred to as modified Wilson and Cooke (MWAC) samplers (Mendez et al., 2011;Wilson and Cooke, 1980) and consist of a closed Polyethylene bottle through which the wind can pass via two glass tubes of 8 mm openings. Thus, a big difference between the traps and the MWAC collectors is the much smaller collection area of the MWAC collectors with 44 mm^2. The MWAC dust sampler was chosen because it is one of the most common (Zobeck et al., 2003) and most efficient dust samplers (Goossens and Offer, 2000). The sampling bottles were mounted horizontally at five different heights.

The samples collected in 2013-2015 were chosen for subsequent flux and grain-size analyses (Table 4). Saltating dust particles may be collected in the lower sampling bottles at 90 cm. However, the aim was to analyse dust transported in suspension to enable a better comparison between the continental and marine sites. Therefore, the highest sampling bottles attached to the mast at 2.90 m height were used for microscope, flux and grain-size analysis (Table 4). One series of bottles (series B2) of mast 2 were analysed with the microscope. The other three replicate samples (bottles A1 and B1 of mast 1, bottles A2 of mast 2) were analysed for flux and grain-size analysis. Out of the three replicate samples, the sample with the highest mass was chosen for the interpretation of the flux and grain-size data because this bottle was assumed to have sampled most efficiently. Three samples mounted at a height of 2.40 m of mast 2 were chosen to test the effect of the chemical pre-treatments that we do to isolate the terrigenous fraction from marine sediments on the resulting grain-size distributions (Fig. 2). Two winter and two summer samples that contained enough material were chosen for XRD measurements (Table 3).

Furthermore, dust was sampled with a MWAC dust sampler mounted on the mast of buoy Carmen, at about 2 m above the sea surface (Stuut et al., 2015). The masts of the buoy Carmen and of the Iwik dust sampler were aligned to the ambient wind direction via a wind vane (Fig. 2). This MWAC dust sample was also analysed for grain-size distribution.

Table 4: Specifications of the MWAC samples collected during 2013-2015 chosen for flux and grain-size analysis.

Dust collector series	Trap type	Sampling period	Position	Height [m]	No. of samples	Sampling intervals
Iwik 13	MWAC	27.01.2013 – 20.01.2014	19°53.1' N 16° 17.6' W	2.90	11	19 d, 28 d. 32 d, 29 d, 40 d, 21 d, 31 d, 61 d, 31 d, 31 d, 35 d
Iwik 14	MWAC	20.01.2014 - 18.01.2015	19°53.1' N 16° 17.6' W	2.90	13	26 d,. 28 d, 31 d, 30 d, 31 d, 30 d, 31 d, 31 d, 30 d, 32 d, 29 d, 34 d
CB-MWAC	MWAC	23.08.2014 – 16.11.2015	21°15.8' N 20°56.1' W	2.00	1	450 d

2.3 Microscopy

The MWAC samples chosen for microscopic investigation were analysed with a Leica M165 C microscope. Microscope pictures were taken using a Leica DFC420 camera attached to the microscope. The software Leica application suite 3.8 was used for taking the pictures.

2.4 Dust and lithogenic fluxes

1/5 splits of the sediment trap samples were analysed for dust fluxes and the bulk components following the method presented in Fischer and Wefer (1991). The lithogenic flux [$mgm^{-2}d^{-1}$] was estimated according to Eq. (1):

$$lithogenic\ material = dust = total\ mass - carbonate - opal - 2\ x\ Corg \quad (1)$$

Organic carbon was measured after the removal of carbonate with 2N HCl using a CHN-Analyser (HERAEUS). Total carbon was estimated by combustion without pre-treatment. Carbonate was determined according to Eq. (2):

$$carbonate = total\ carbon - organic\ carbon \quad (2)$$

Biogenic opal was determined with a sequential leaching technique (Müller and Schneider, 1993).
The MWAC samples chosen for dust flux analyses were weighed on a Mettler-Toledo AT261 Delta Range balance with a precision of 0.0001 g. Mean atmospheric dust concentrations were estimated as Eq. (3):

$$\mathrm{DL} = \frac{MAR}{(v*A)} * \frac{1}{\eta} \quad (3)$$

Where DL is the mean dust concentration [μgm^{-3}], MAR is the mass accumulation rate [μgs^{-1}], v is the mean wind speed per sampling month [ms^{-1}], A is the cross-sectional area of the inlet tube of the MWAC sampler [m^2] and η is the estimated sampling efficiency of MWAC bottles. A sampling efficiency of 90 % was assumed based on an efficiency study of Goossens and Offer (2000). Mean horizontal dust fluxes were calculated according to Eq. (4):

$$F_h = \frac{MAR}{A} * \frac{1}{\eta} \quad (4)$$

where F_h is the horizontal dust flux [$mgm^{-2}d^{-1}$], MAR is the mass accumulation rate [mgd^{-1}], A is the cross-sectional area of the inlet tube of the MWAC sampler [m^2] and η is the estimated sampling efficiency of MWAC bottles.

2.5 Particle size

A 1/25 split of the marine sediment trap samples was analysed for particle size of the terrigenous fraction. The samples were pre-treated before measurement in order to isolate this fraction (see also Filipsson et al. (2011);Friese et al. (2016), Meyer et al. (2013) and Stuut (2001) for methodology) with the following steps: (1) removal of organic matter: Addition of 10 ml of H_2O_2 (35%) to the sediment sample and subsequent boiling until the reaction stops, (2) removal of calcium carbonate: Addition of 10 ml HCl (10%) to the sediment sample and subsequent boiling for exactly 1 minute and (3) removal of biogenic silica: Adding 6 g of NaOH pellets to the sediment sample and subsequent boiling for 10 minutes. Before particle-size analysis, 10 drops of $Na_4P_2O_7*10H_2O$ were added to each sample to assure the full disaggregation of the particles. The pre-treatment of the MWAC samples differed from the pre-treatment of the sediment trap samples as, obviously, these samples did not contain any biogenic material originating from marine plankton. Further, the disaggregation of particles needed to be kept at minimum to allow for the study of dust transport processes, the so-called 'minimally dispersed' aeolian fraction (McTainsh et al., 1997). Therefore, the MWAC samples were solely pre-treated with three drops of $Na_4P_2O_7*10H_2O$ before analysis. The marine sediment-trap samples as well as the MWAC samples were analysed with the laser particle sizer Beckmann Coulter LS13320 at NIOZ using a Micro Liquid Module (MLM). This instrument allows quick, accurate, and precise data acquisition of large size intervals (Bloemsma et al., 2012). An analytical error of ± 1.26 µm (± 4.00 %) was considered for the measurements (Friese et al., 2016).

To investigate the comparability of the MWAC samples with the oceanic sediment-trap samples, the particle-size distribution of the MWAC sample attached to buoy Carmen was compared to the averaged particle-size distributions of the upper and lower trap series at site CB (Fig. 3a). The grain-size distribution of the MWAC sample was comparable to both sediment trap time series even though the sampling time period was different. To ensure that the pre-treatment steps of the traps did not influence the terrigenous fraction itself, tests were made in which the on-land MWAC samples were exposed to the same pre-treatment steps as the marine samples (Fig. 3b).

One spring sample has been measured with and without a chemical pre-treatment. Two fall dust samples were obtained from the same height and mast and sampling interval, however from different bottles (A and B) and were measured with and without pre-treatment. The figure indicates that a pre-treatment of the Iwik dust samples did not alter the particle distributions of the samples significantly. Further, the particle-size distribution of dust sampled with different bottles is comparable.

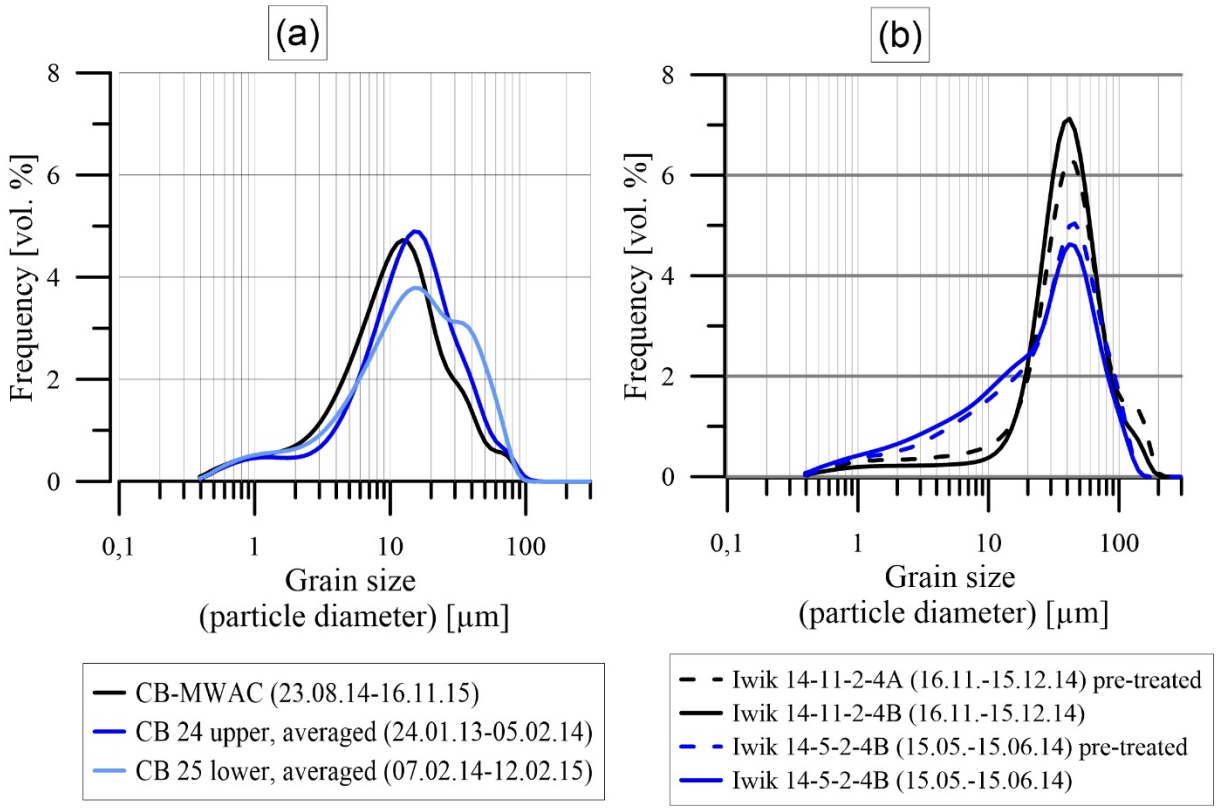

Figure 3: (a) Grain-size distributions for the station CB: Dust sampled with the MWAC sampler 2 m above sea level, with the upper sediment trap at 1214 mbsl and the lower trap at 3622 mbsl. (b) Grain-size distributions of samples of the Iwik 14 time series which have been pre-treated with HCl, H_2O_2 and NaOH (dotted lines) and without pre-treatment (lines).

2.6 Mineral assemblages

Two winter and two summer samples of the MWAC dust collector and the sediment-trap series CBi were chosen for XRD analysis (Table 3). X-Ray Diffraction pattern analyses were carried out in the laboratory of the research group Crystallography (University of Bremen, Central Laboratory for Crystallography and Applied Material Sciences, ZEKAM, Dept. of Geosciences).

Due to the small amount of material in the available dust samples (< 100 mg), the preparation for the measurement was done by pipetting a demi-water-sample mixture on glass slides. A thorough preparation commonly increases reproducibility of the results, however, the standard deviation given by Moore and Reynolds (1989) of ±5% can be considered as a general guideline for mineral groups with >20% clay fraction. In addition, the determination of well-crystallized minerals like quartz, calcite or aragonite can be done with better standard deviations (Tucker and Tucker, 1988;Vogt et al., 2002). The X- Ray Diffraction was measured on a Philips X'Pert Pro multipurpose diffractometer equipped with a Cu-tube (k$_{\alpha}$ 1.541, 45 kV, 40 mA), a fixed divergence slit of ¼°, a secondary Ni-

Filter and the X'Celerator detector system. The measurements were carried out as a continuous scan from 3 – 85° 2θ, with a calculated step size of 0.016° 2θ (calculated time per step was 100 seconds). Mineral identification was accomplished using the Philips software X'Pert HighScore™, which, besides the mineral identification, can give a semi-quantitative value for each identified mineral on the basis of Relative Intensity Ratio (R.I.R.)-values. The R.I.R.-values are calculated as the ratio of the intensity of the most intense reflex of a specific mineral phase to the intensity of the most intense reflex of pure corundum (I/Ic) referring to the "matrix-flushing method" after Chung (1974). Unfortunately R.I.R. values are sparse for clay minerals and long chain organic materials hampered the quantification of our samples.

2.7 Meteorological data

The obtained flux and size data were compared to near-by meteorological data (wind speed, wind direction and precipitation).

Wind direction, wind speed and precipitation data with a 20 minute resolution were gathered for the sampling site CB (21°17' N – 21°12' N, 20°56' W - 20°54' W) during the buoy Carmen deployments from November 2013 to September 2015 with a Vaisala WXT520 meteorology sensor. The size of the dataset was reduced by calculating four hour averages. Moreover, wind direction and wind-speed data with a resolution of five minutes to one hour were gathered during sampling at site Iwik (19°53.1' N, 16° 17.6' W) from January 2013 to January 2015 with a Davis 6250 Vantage Vue meteorology sensor. The size of the dataset was reduced by calculating one-hour averages. Further hourly precipitation data were gathered from the station Arkeiss (20° 7' N, 16° 15' W) from December 2013 to March 2015 with another Davis 6250 Vantage Vue meteorology sensor. Continental hourly wind direction and wind-speed data was acquired for the Nouadhibou meteorological station (20° 55' N, 17° 1' W) online from the Cedar Lake Ventures website (https://weatherspark.com).

Local daily precipitation data (TRMM 3B42 dataset, 0.25° spatial resolution) were derived from the Giovanni online data system, developed and maintained by the NASA GES DISC (http://gdata1.sci.gsfc.nasa.gov). Daily precipitation data were downloaded as area-averages around CBi (20° 58' N - 20° 34' N, 18° 56 W - 18° 32' W), Iwik (19° 41' N - 20° 5'N, 16° 29' W - 16° 05' W), CB/Carmen (21° 05' N - 21° 29' N, 21° 02' W - 20° 38' W) and Arkeiss (20° 19' N - 19° 55' N, 16° 28' W - 16° 04' W) according to the assumed catchment area of the upper trap (~ 40 x 40 km^2).

Maps of six hourly mean surface wind vectors and speed (20^{th} century reanalysis V2c dataset) were provided by the NOAA/OAR/ESRL PSD, (Boulder, Colorado, USA) and downloaded from their website (http://www.esrl.noaa.gov/psd/).

2.8 Mapping with ArcMap

The mapping software ArcMap version 10.3.1 was used to analyze the source regions of the dust samples investigated for mineralogical composition. A map was created with four-day back-trajectories for days with a dust-storm event as depicted on satellite images. In addition, the African surface lithology was included in the map and soils rich in the minerals calcite, kaolinite and chlorite were marked.

371 Satellite quasi-true colour RGB images (MODIS dataset) were retrieved from the NASA Worldview website
372 (https://worldview.earthdata.nasa.gov).

373 Four-day back trajectories at altitudes of 10 (following Stuut et al. (2005)), 100, 3000, 4500 (following Skonieczny
374 et al. (2013)) and 5500m were calculated ending at the dust collector site Iwik (19°52' N, 16°17' W) and at the
375 proximal marine trap site CBi (20°46',18°44' W) using the Hybrid Single Particle Langrangian Integrated
376 Trajectory (HYSPLIT) model (Stein et al., 2015) and the reanalysis dataset (2.5° spatial resolution) on the NOAA
377 website (http://ready.arl.noaa.gov).

378 An ArcGIS layer file of the African surface lithology
379 (new_af_lithology_w_glbcvr_waterbdy_90m_dd84_final.lyr) was downloaded from the U.S. Geological survey
380 (USGS) website (http://rmgsc.cr.usgs.gov).

381 An ArcGIS shape file of the African soils (DSMW.shp) was downloaded from the website of the food and
382 agriculture organization of the United Nations (FAO) (http://www.fao.org). The mean percentage of calcite (8.9
383 %), chlorite (4.1 %) and kaolinite (29%) in the clay fraction of Saharan soils in general and for each soil type is
384 given by Journet et al. (2014). Soils with larger percentages of calcite, chlorite or kaolinite in the clay fraction than
385 the average percentages were marked in the ArcGIS map.

386

387

3. Results

3.1 Meteorology

In Fig. 4 the meteorological data of the sites Carmen (CB), CBi, Iwik, Arkeiss and Nouadhibou during 2013 to 2014 are presented (see Fig 4a for location of the sites). The rainfall frequency is given in Fig. 4b for each site. The number of rainfall events were calculated regarding the TRMM stations for precipitation rates >1 mmd^{-1} because smaller precipitation amounts which were detected by the satellite may not actually reach the ground. Regarding the surface stations Carmen and Arkeiss, a threshold of >0.2 mmd^{-1} was used in order to exclude events which may be related to anomalously high moisture instead of rainfall.

According to the TRMM satellite product the annual precipitation frequency was larger on the shoreline (station Arkeiss and Iwik) than offshore (station CBi and Carmen) (Fig. 4b). This may be explained by a decrease in atmospheric water vapor content due to precipitation when the winds move westward. Moreover, the TRMM satellite product indicated larger rainfall frequencies during the summer season compared to the winter season regarding the stations Carmen, CBi, Iwik and Arkeiss. Larger summer rainfall frequencies can be explained by the summer northward shift of the ITCZ to ~ 21° N resulting in more frequent moist convection and rainfall in the study area.

The annual rainfall frequency at the site Arkeiss and the summer rainfall frequencies at the sites Arkeiss and Carmen compare quite well between the sensors and the TRMM observations. However, the spatial and seasonal trends observed by the TRMM data were not supported by the sensor on buoy Carmen and by the surface station in Arkeiss. The larger annual and winter rainfall frequency recorded with the sensor on buoy Carmen may be related to water emission from the ocean surface during time periods with strong surface winds. Further, disagreements between the surface stations and the TRMM stations may be caused by the local signal recorded by the respective rain sensor. A larger number of rain sensors would most likely improve the comparability to the TRMM data.

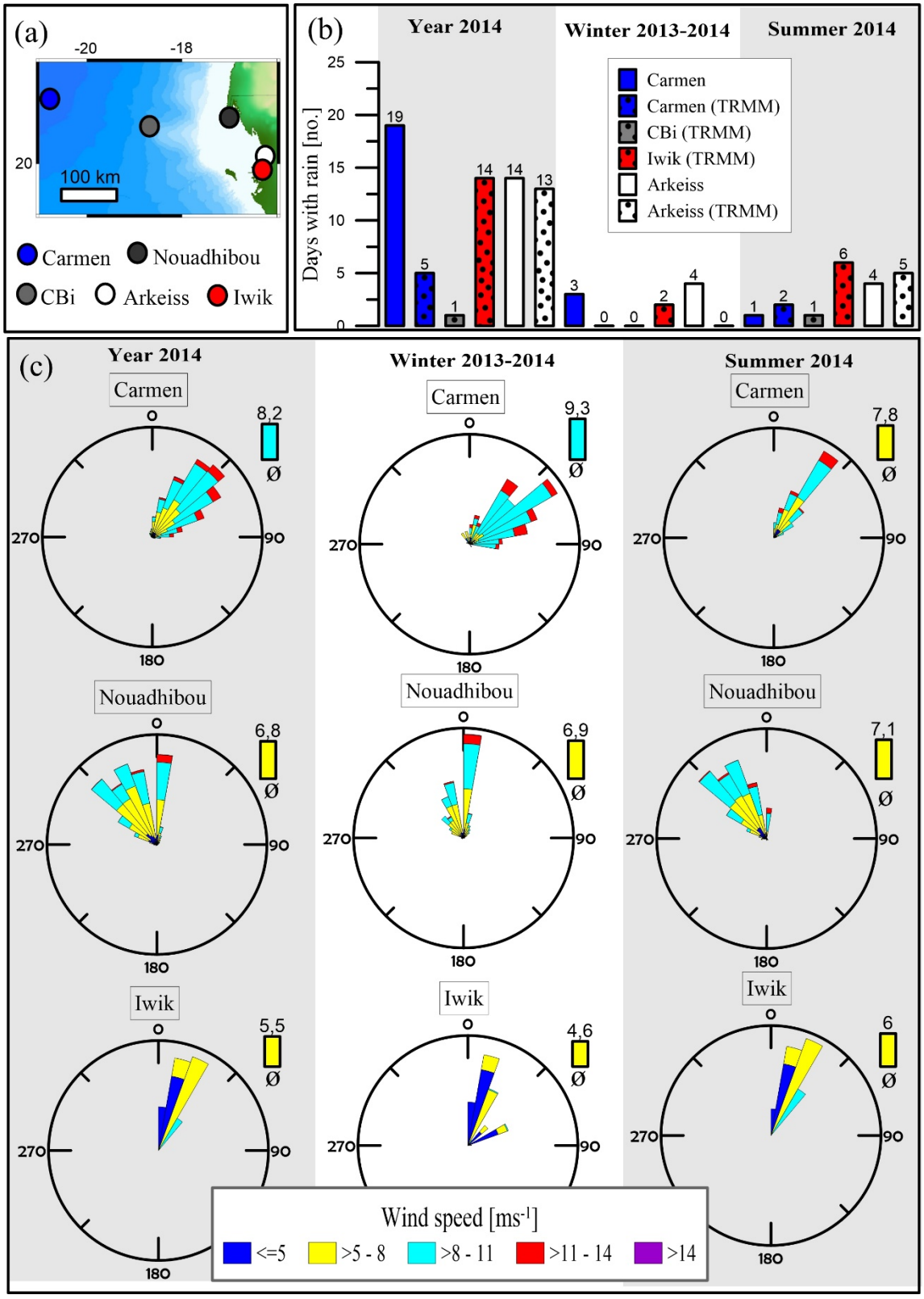

Figure 4: Meteorological data: (a) map showing the sites Carmen (CB), CBi, Iwik, Nouadhibou and Arkeiss under investigation (b) precipitation at the sites Carmen (CB), CBi, Iwik and Arkeiss (c) wind direction and speed at the sites Carmen (CB), Nouadhibou and Iwik.

The wind direction and speed for the surface stations Carmen, Nouadhibou and Iwik are displayed in Fig. 4c. The annual average surface wind velocity was maximum offshore at buoy site Carmen (CB) with ~ 8 m/s. The buoy

recorded a larger average wind velocity during winter than during summer, which is consistent with this season being dominated by the Trades. On the shoreline, the average wind velocity was slightly larger during summer than during winter. The predominant annual wind direction was NE at site Carmen and Iwik, while predominant NW winds were recorded for the site Nouadhibou. The wind direction changed from predominant NE during winter to predominant NNE direction during summer at site Carmen. A similar, but less pronounced seasonal trend can be observed for the continental site Iwik. In Nouadhibou, the predominant winter wind direction is NNW switching to a predominant NW wind direction during summer. Obviously, with winds originating from the open ocean, not a lot of dust is anticipated. Therefore, we interpret these wind directions as being very local and caused by the shape of the peninsula of Cape Blanc.

3.2 Microscope findings of the dust samples from Iwik

In Fig. 5 the results of the microscopy investigation of the Iwik 2013 time series are presented. In general, the majority of the particles consisted of angular and moderately spherical quartz grains with a diameter of ~ 50 µm (Fig. 5a,b). A small percentage of large platy minerals with a diameter of ~ 200 µm were found in all samples (Fig. 5b). Large quartz grains with a diameter of ~ 150 to 200 µm were detected in 45 % of the samples. An anomalously high percentage of sub-angular and moderately spherical quartz grains with an average diameter of ~ 200 µm was observed in one summer sample (Fig. 5c). Aggregated grains occurred in all samples. However, the percentage and size of the aggregates as well as the size of the aggregated grains differed from sample to sample. Usually, the size of the aggregated grains was ~ 50 µm (Fig. 5a). Two samples were characterized by aggregates composed of particles with a smaller size of ~ 20 µm (Fig. 5d).

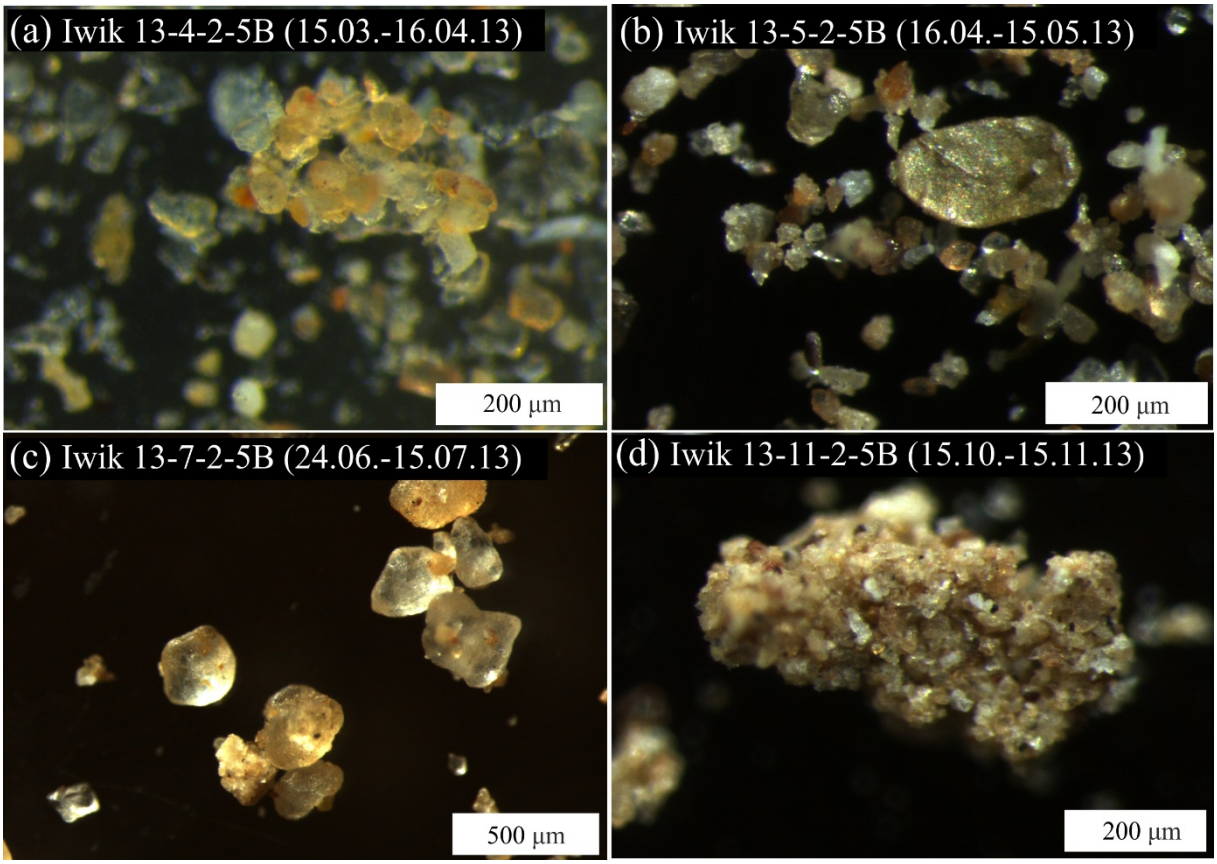

Figure 5: Microscopic photographs of selected dust samples from the Iwik 2013 time series. (a) Spring dust sample with a ~ 250 x 150 µm aggregate, (b) spring dust sample with a ~ 200 x 100 µm mica chip, (c) summer dust sample with ~ 200 x 200 µm quartz grains, (d) fall dust sample with a ~ 600 x 250 µm aggregate.

3.3 Dust fluxes and size on land and in the ocean

In Table 5 the average dust fluxes are given for the sampling sites Iwik, CBi and CB. The dust concentrations at site Iwik were determined based on the measured wind speed of the meteorological sensor attached to the sampling mast. For four samples no wind data were available due to a failure of the instrument. For these samples a wind velocity was assumed based on the seasonal averages calculated from the available wind data of the meteorology sensor in Iwik (Fig. 4c). The annual average horizontal dust fluxes at site Iwik were of the same order of magnitude during 2013 and 2014. The annual average dust fluxes decreased from the on-land site Iwik towards the proximal site CBi and the distal site CB. At the site Iwik the average dust concentration was maximum during spring plus winter 2013 and 2014 with 393 μgm^{-3} and 341 μgm^{-3}, respectively, and minimum in fall 2013 and 2014 with 48 and 68 μgm^{-3}, respectively. The dust fluxes generally decreased with collection height in the mast between 90 and 290 cm (not shown).

Table 5: Seasonal and annual average dust fluxes and average modal grain size, mean/mode ratio and standard deviation of the grain-size distributions from Iwik 13-14, CBi 11-12 upper and CB 24 upper time-series.

Series	Year	Winter	Summer	Annual
Average dust fluxes [$mg.m^{-2}.d^{-1}$] (dust concentration [$\mu g.m^{-3}$])				
Iwik 13	2013	10000 (30)	113000 (268)	95000 (214)
CBi 11 upper	2013	106	168	99
CB 24 upper	2013	53	44	45
Iwik14	2014	208000 (603)	55000 (127)	102000 (275)
CBi 11+12 upper	2014	98	20	47
Average modal grain size [µm]				
Iwik 13	2013	44	49	48
CBi 11 upper	2013	27	39	29
CB 24 upper	2013	16	17	16
Iwik 14	2014	45	49	48
CBi 11+12 upper	2014	34	44	33
Average mean/mode ratio [µm]				
Iwik 13	2013	0.7	0.6	0.6
CBi 11 upper	2013	0.5	0.3	0.5
CB 24 upper	2013	0.7	0.8	0.7
Iwik14	2014	0.6	0.4	0.6
CBi 11+12 upper	2014	0.5	0.3	0.5
Average standard deviation [µm]				
Iwik 13	2013	2.8	3.1	3.0
CBi 11 upper	2013	3.0	3.3	3.1
CB 24 upper	2013	2.7	2.6	2.6
Iwik 14	2014	2.8	3.5	3.1
CBi 11+12 upper	2014	3.1	3.3	3.0

The statistical values of the measured grain-size distributions for the stations CB, CBi and Iwik are given in Table 5. In addition, the measured grain-size distributions for the time series of the stations CB, CBi and Iwik are displayed in Fig. 6. In Fig. 6a the average grain-size distribution for the samples of each of the three stations for the year 2013 are given. The maximum measured particle size decreased from ~223 µm on land at site Iwik to

~169 µm at the proximal site CBi and ~140 µm at the distal site CB (Fig. 6a). In addition, the average modal grain size decreased from ~48 µm at site Iwik to 16 µm at site CB (Table 5). Bimodal grain-size distributions were encountered for 23 % of the CBi 11-12 samples, 13 % of the Iwik 13-14 samples, and none of the CB 24 samples. The three bimodal distributions of the Iwik 13-14 time series were characterized by an additional fine mode peaking at ~16 µm besides the more pronounced and variable coarse mode peaking at ~42 to 55 µm. The three Iwik dust samples characterized by a fine grain-size peak were collected during spring, summer (Fig. 6c) and fall. The eight bimodal grain size distributions of the CBi 11-12 time series were characterized by a variable coarse mode at ~ 25 to 35 µm and a variable fine mode at ~ 6 to 16 µm. The standard deviation of a grain-size distribution is a measure of the sorting of the dust sample: the larger the standard deviation the weaker the sorting. The sorting of the CB samples was better than the sorting of the Iwik and CBi time series as indicated by the average geometric standard deviations of 2.6 µm for CB and 3.1 µm for both Iwik and CBi (Table 5). The lowest average mean/mode ratio was recorded for the CBi time-series with ~0.5 due to the weak sorting of the samples (Table 5).

In Fig. 6b-c the measured grain-size distributions for winter and summer samples are displayed. The averaged modal grain size for the summer samples was coarser grained compared to the winter samples of the respective grain-size time series (Table 5). The seasonality in modal grain size was largest for the CBi 11 upper trap series of the year 2013 with a difference of ~12 µm (Table 5). The average standard deviation was larger and the average mean/mode ratio was smaller in the summer samples compared to the winter samples regarding the sites Iwik and CBi (Table 5). In other words: the summer samples of sites CBi and Iwik were less well sorted (Fig. 6b and c). This seasonal trend was not observed in the CB 24 upper samples which were generally well sorted (Table 5).

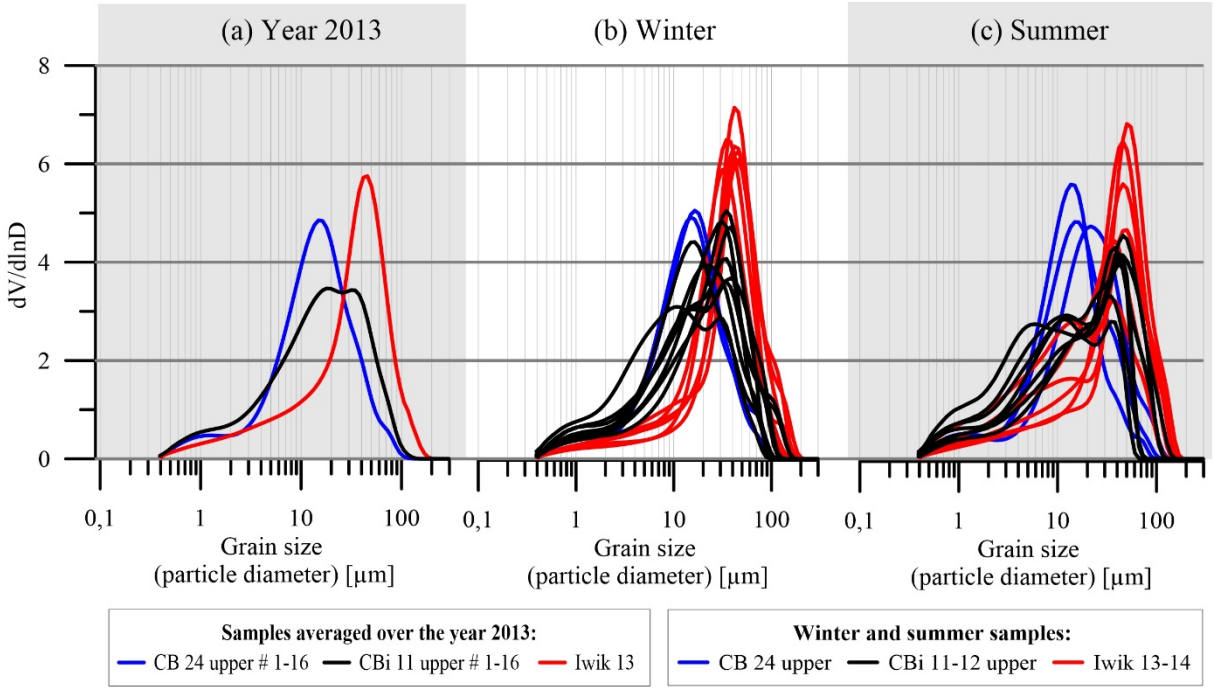

Figure 6: Grain-size distributions of the stations Iwik, CBi and CB (a) averaged for the samples of the year 2013 (b) winter samples (c) summer samples.

In Fig. 7a –c the results of the correlation between the characteristics of the dust sampled on land and the local meteorological data are presented. In Fig. 7a the particle sizes were correlated to the surface wind speed data (N = 13 samples). A correlation above a coefficient of determination (R^2) of 0.3 was considered significant at the 95 %

confidence level for two-tailed probabilities. The modal particle size of the Iwik samples showed a positive linear correlation with the daily wind speed events with $R^2 = 0.5$, which is significant at the 99.31 % confidence level. The correlation was only evident when using a threshold for wind events of 3.5 to 5.5 ms^{-1} and was best for a threshold of 5 ms^{-1}. A better positive linear correlation was obtained when excluding the spring sample resulting in $R^2 = 0.7$ which is significant at the 99.96 % confidence level.

In Fig. 7b the dust fluxes were correlated to the surface wind-speed data (N = 10 samples). A correlation above $R^2 = 0.4$ was considered significant at the 95 % confidence level for two-tailed probabilities. The horizontal dust flux of the Iwik samples correlated positively to the daily wind speed events during the sampling interval with $R^2 = 0.7$ which is significant at the 99.75 % confidence level. The correlation was only evident when using a threshold for wind events of 6.5 to 7 ms^{-1} and was best for a threshold of 6.5 ms^{-1}. Moreover, a significant linear correlation with $R^2 = 0.6$ was observed at the 99.15 % confidence level between the dust fluxes and the mean wind strengths during the sampling intervals (not shown).

In Fig.7c the particle size of the Iwik summer samples was correlated to the local TRMM precipitation data (N= 6 samples). In this case a correlation above $R^2 = 0.7$ was considered significant at the 95 % confidence level for two-tailed probabilities. A good linear negative correlation with $R^2 = 0.9$ was observed which is significant at the 99.78 % confidence level.

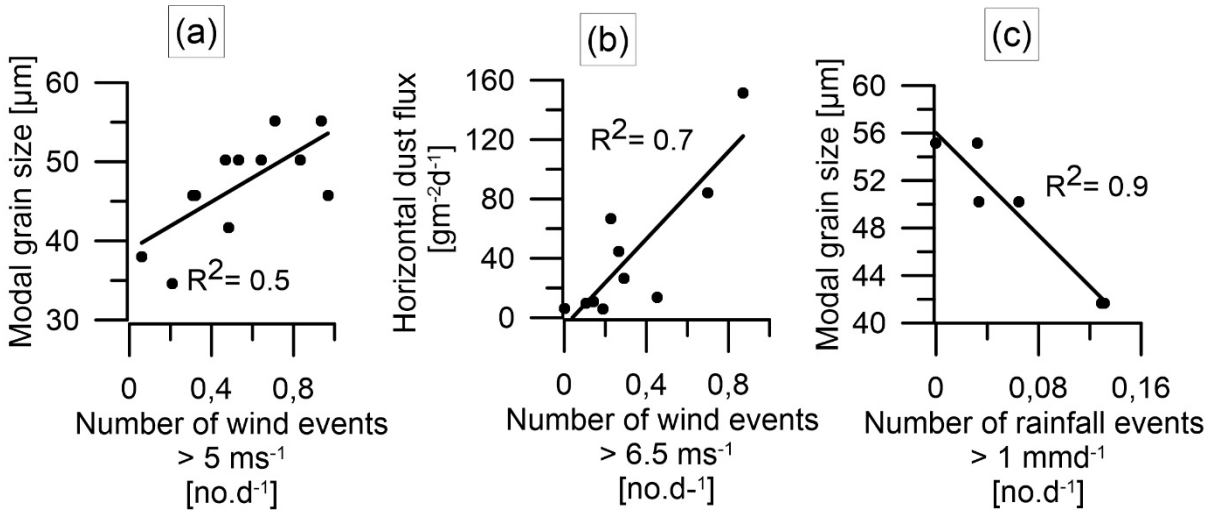

Figure 7: Correlation between the observed local surface wind speed at site Iwik and the measured (a) modal grain size and (b) flux. (c) Correlation between the observed local precipitation at site Iwik (TRMM data) and the modal grain size of the summer samples.

3.4 Mineral assemblage of dust sampled on land and in the ocean

In Table 6 the mineralogical composition averaged over all eight samples, averaged over the four Iwik samples and the four CBi samples is given. All dust samples contained the minerals quartz and mica. Further minerals that occurred with significant quantities but which were not present in all dust samples were feldspar, amphibole, zeolite, chlorite and palygorskite. Calcite, dolomite, gibbsite, kaolinite, smectite, sepiolite, fluellite, anhydrite, rutile and serpentine occurred only in some samples resulting in a low average abundance ≤ 1%. However, we argue that these minerals can be used as dust source indicators because of (1) the characteristic distribution of gibbsite, kaolinite, smectite and sepiolite in North Africa according to different weathering regimes (Biscaye,

1964) and (2) the characteristic occurrence of fluellite, anhydrite, rutile and serpentine according to outcropping rock type (Deer et al., 1992). Further minerals that occur in low abundances (≤ 3%) were summarized as 'other minerals' and will not be discussed in the manuscript. While the continental samples were dominated by quartz and feldspar, the marine samples were dominated by mica, followed by quartz and feldspar.

Table 6: Results of the mineralogical investigation: Mineral assemblage averaged over all samples (Total), the Iwik samples (Iwik) and the CBi samples (CBi).

*	Qz [%]	Fsp [%]	Mi [%]	Amf [%]	Pal [%]	Chl [%]	Cc [%]	Dol [%]	Gib [%]	Zeo [%]	Kao [%]	Sme [%]	Se [%]	Rut [%]	Serp [%]	Ga [%]	Anh [%]	Flu [%]
Total	25.1	21.5	25.5	5.1	3.4	4.4	0.6	0.1	1.0	3.8	0.9	0.4	1.1	0.5	0.3	0.1	0.1	1.1
Iwik	33.3	30.8	18.0	5.0	3.3	1.8	1.3	0.3	2.0	0.0	0.0	0.0	0.0	0.8	0.5	0.0	0.0	0.0
CBi	17.0	12.3	33.0	5.3	3.5	7.0	0.0	0.0	0.0	7.5	1.8	0.8	2.3	0.3	0.0	0.3	0.3	2.3

*Qz = quartz, Fsp = feldspar, Mi = mica, Amf = amphibole, Pal = palygorskite, Chl = chlorite, Cc = calcite, Dol = dolomite, Gib = gibbsite, Zeo = zeolite, Kao = kaolinite, Sme = smectite, Se = sepiolite, Rut = rutile, Serp = serpentine, Ga = garnet, Anh = anhydrite, Flu = fluellite

In Fig. 8a-c the results of the mineralogical investigation of the eight chosen dust samples are presented. Figure 8a depicts again the average composition of the samples per sampling site (N=4). The minerals zeolite, anhydrite, garnet, sepiolite, fluellite, kaolinite and smectite were only found in the marine samples. Only the continental sample of 15.08.-15.09.14 contained traces of zeolite. While gibbsite, serpentine, calcite and dolomite were detected in the continental dust samples, these minerals were absent in all marine samples. The absence of calcite and gibbsite may have been caused by the pre-treatment of the marine sediment-trap samples with HCl. Although the concentration of the used acid is fairly low (10%) and the exposure time of the samples was exactly 1 minute, we cannot exclude that carbonate minerals were dissolved. Therefore, the absence of these minerals in the marine traps will not be discussed further.

In the following, the seasonality in the average mineralogical composition will be outlined for each site as given in Fig. 8b,c. At site Iwik, the winter dust samples were characterized by the occurrence of chlorite, serpentine and rutile, while the summer samples were characterized by the minerals gibbsite and dolomite. At site CBi, the winter dust samples were characterized by the occurrence of the minerals sepiolite, fluellite, kaolinite, smectite, garnet and anhydrite, while the summer samples were characterized by the mineral rutile. Only for the marine trap samples an annual average chlorite/kaolinite ratio (C/K = 4) could be derived owing to the occurrence of kaolinite.

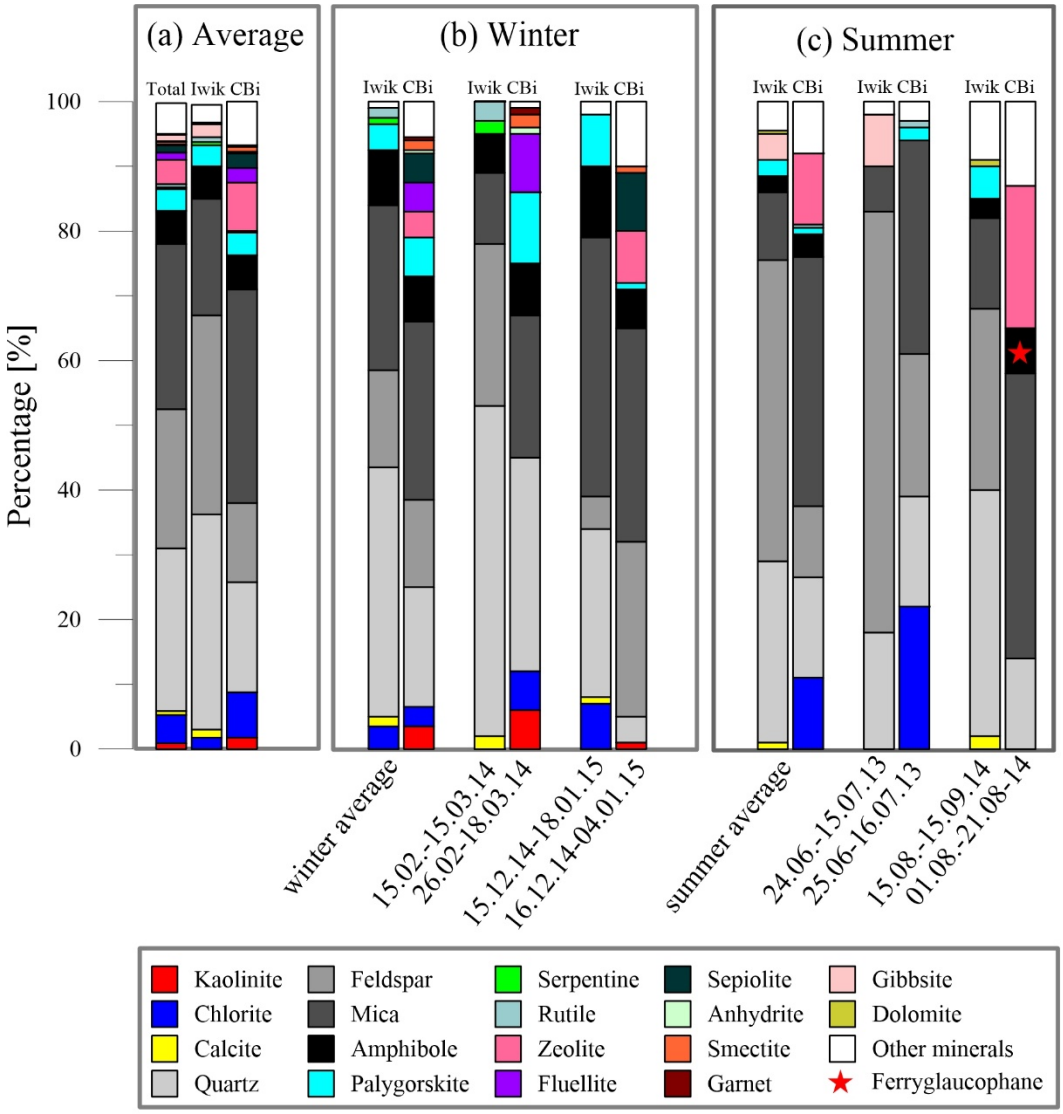

Figure 8: Mineralogical composition (a) averaged over all samples and for sites Iwik and CBi, (b) averaged for the winter samples at sites Iwik and CBi and for each individual winter sample and (c) averaged for the summer samples at sites Iwik and CBi and for each individual summer sample. The category 'other minerals' comprises the minerals todorokite, sodalite, konicklite, guyanaite, nitratnine, urea, bernalite, akermanite, mixed-layer clay and talc.

3.5 Identification of dust source regions

In Fig. 9-12 the results of the four day back-trajectory analysis are presented for each sample which has been analyzed for mineralogical composition. Four heights, 10, 100, 3000 and 4500 m were chosen to cover both low- (trades) and high-level (SAL) dust transport. A back trajectory was drawn for the day when a dust storm event occurred as depicted on the satellite images. Only the low-level back-trajectories were plotted for site Iwik because of the correlation of the measured dust characteristics to the low-level wind speed. Moreover, the MWAC samplers were designed to only sample dry deposition, whereas the marine sampling sites collect material settling through the water column, i.e., dust resulting from both dry- and wet deposition. The back-trajectories at 5500 m can be found in the supplement.

553 Figure 9 illustrates a typical late-winter situation. During the sampling interval of each site at least two days with
554 dust storms occurred (Fig. 9c,d). Therefore, two back trajectories were drawn for each height for the site CBi and
555 CB respectively. The high-level back trajectories ending at site CBi pass either through the major **PSA 2** or point
556 offshore. Both the low-level back-trajectories ending at the continental trap site Iwik and at the oceanic trap site
557 CBi point to a dust source within the major **PSA 2** (Scheuvens et al., 2013). Some calcite was present in the
558 continental dust sample, but no chlorite nor kaolinite was detected. Therefore, the dust source was most likely
559 located in the nearby southwestern Reguibat Shield where sediments are rich in calcite and quartz and depleted in
560 chlorite and kaolinite (Fig. 9a). Dust deposited in the marine traps during the time interval was characterized by
561 the occurrence of chlorite and kaolinite. Thus, the source area of the samples was most likely the chlorite and
562 kaolinite rich sediments located near the Bou Craa phosphate mine in the Western Sahara (Fig. 9b).

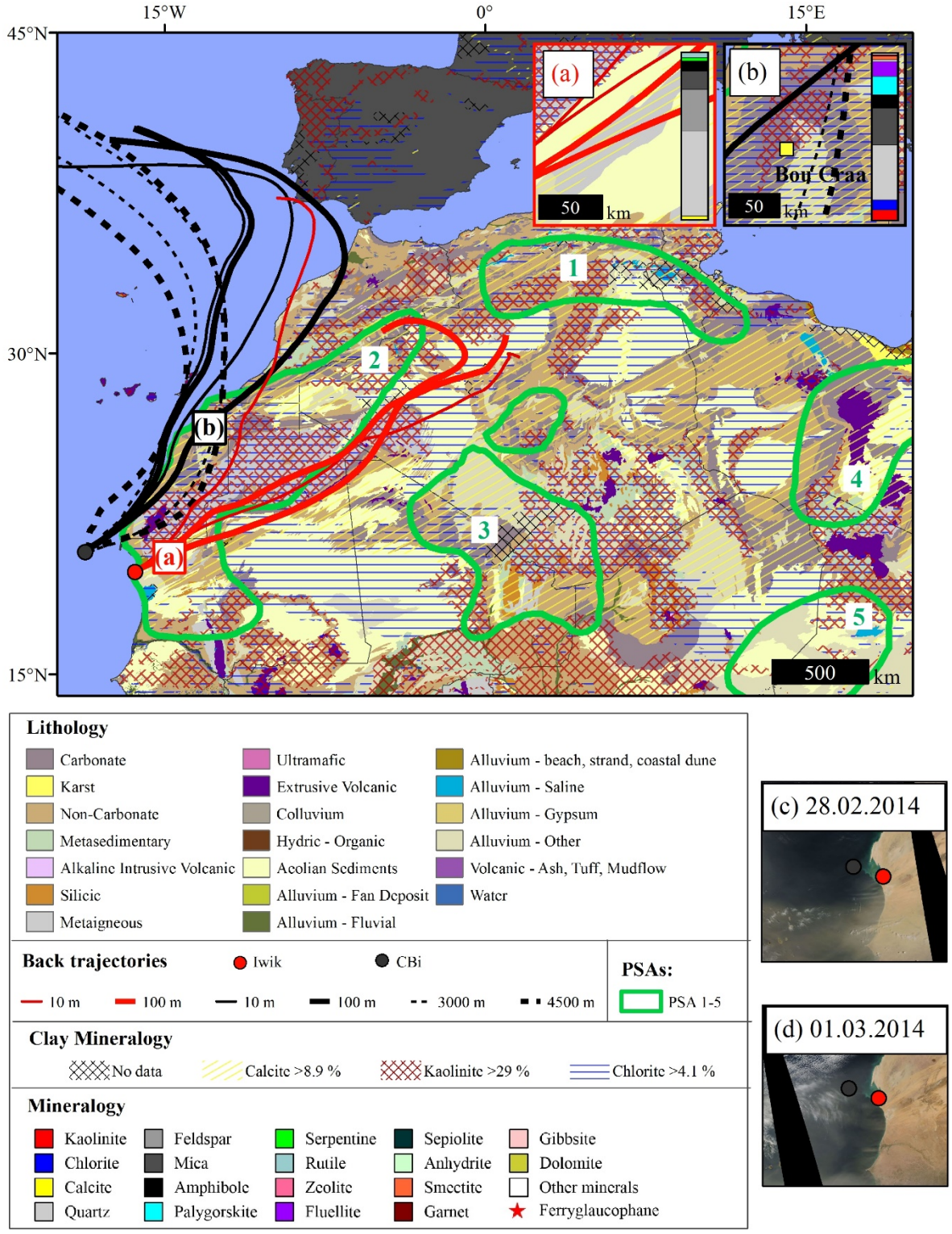

Figure 9: Low-level (10 m) four-day back trajectories of dust events ending during the sampling interval 15.02.-15.03.14 at site Iwik and during the sampling interval 26.02.-18.03.14 at site CBi. The potential dust source areas and the mineralogy of the samples are given in the subfigures a-b. The dust-storm events occurring during the sampling interval are indicated in subfigures c-d.

Figure 10 represents a typical early-winter situation. During the sampling interval of the site Iwik at least three dust storms occurred and at the site CBi at least two dust storms occurred (Fig. 10f-h). Each dust storm lasted for several days for which we could model as many as 15 back trajectories for the site Iwik and 8 for the site CBi for

each height. The large number of back trajectories complicated the determination of the likely source areas. All low-level back trajectories pass through the major **PSA 2** and some point to the **PSA 1** and **PSA 3** (Scheuvens et al., 2013). One high-level back trajectory ending at site CBi passes through PSA 2 and two through Mauritania and Senegal. However most of the high-level back trajectories ending at site CBi predominantly point offshore. Dust sampled in the marine traps during this sampling interval did not contain any chlorite, while the dust trapped at Iwik did. Chlorite may have been supplied to Iwik from a source area nearby the Senegal-Mauritania Basin (Fig. 10a) or as far as the eastern Taoudeni Basin (Fig. 10b) as there are anomalously high chlorite content of the soils in these areas. The continental sample is further characterized by the occurrence of calcite and the absence of kaolinite which fits to the soils of the chosen source areas (Fig. 10a,b). The marine sample was characterized by the occurrence of zeolite and absence of chlorite. Therefore, zeolite may have been derived from the extrusive volcanic rocks of the northern Taoudeni Basin (Fig. 10c). A further source area might be the southern shoreline of the Western Sahara in which chlorite depleted sediments are situated (Fig. 10d). The presence of the mineral kaolinite in this marine winter sample may be explained by a kaolinite-rich source area lying in the southern Senegal-Mauritania Basin (Fig. 10e).

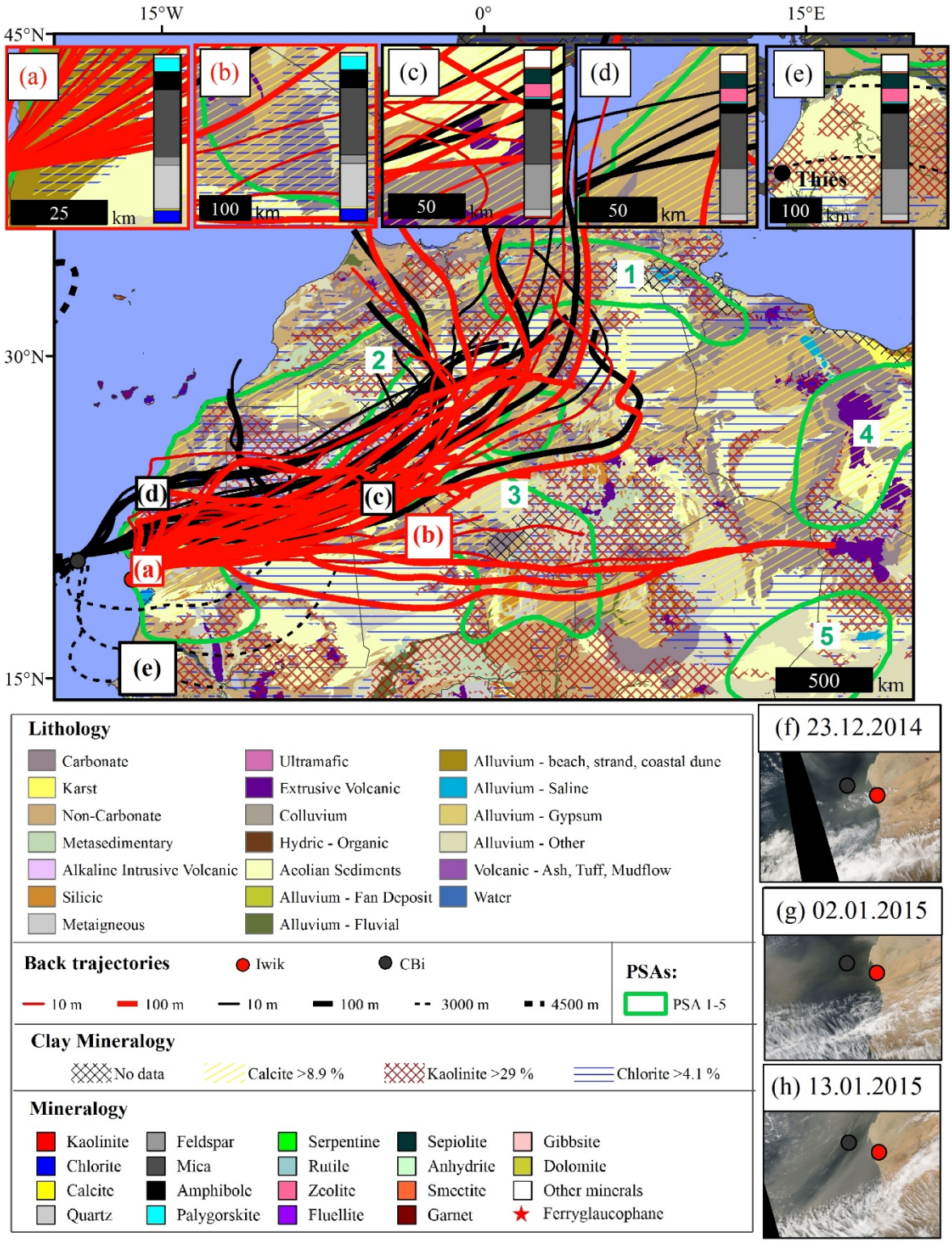

Figure 10: Low-level (10 m) four-day back trajectories of dust events ending during the sampling interval 15.12.14-18.01.15 at site Iwik and during the sampling interval 16.12.14-04.01.15 at site CBi. The potential source areas and the mineralogy of the samples are given in the subfigures a-c. The dust storm events occurring during the sampling interval are indicated in subfigures e-g.

In Fig. 11 a typical early-summer situation is presented. Only one dust storm event was observed during the sampling interval at both sites which lasted for one day (Fig. 11c) resulting in only one back trajectory per site and

per height. The low-level back trajectory ending at site CBi runs offshore. The low-level back trajectory ending at site Iwik passes through the major **PSA 2** and the high-level back trajectory passes through the major **PSA 2**, **3** and **5** (Scheuvens et al., 2013). Dust sampled on land at site Iwik was characterized by the absence of chlorite, kaolinite and calcite which fits to the soils of northern Tidra Island (Fig. 11a) making it a really local phenomenon. In contrast, dust sampled offshore at site CBi was characterized by chlorite and by the absence of kaolinite which fits to the chlorite rich soils in the Mauritanides of Mauritania (Fig. 11b).

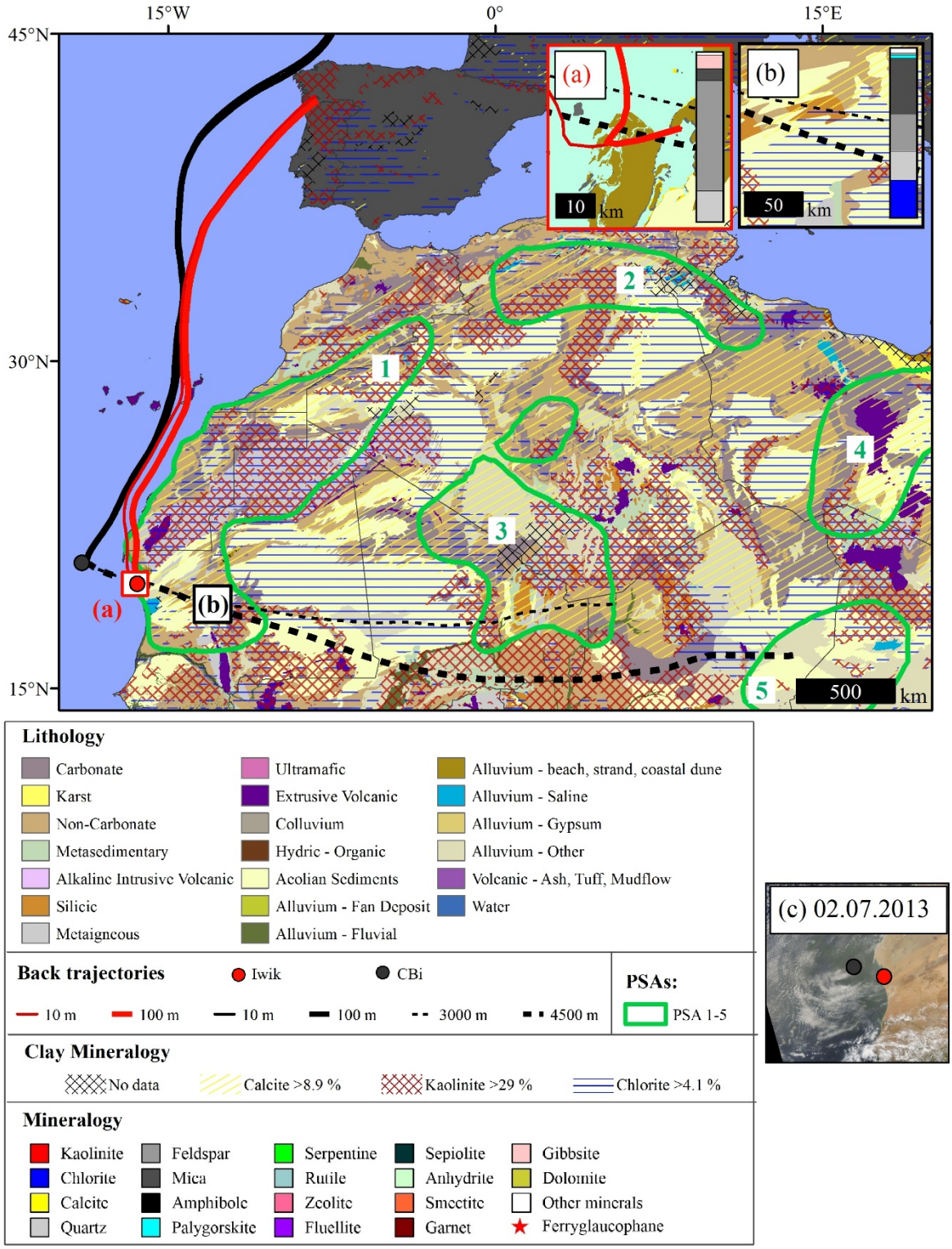

Figure 11: High- (4500 m) and low-level (10 m) four-day back trajectories of a dust event ending during the sampling interval 24.06.-15.07.13 at site Iwik and during the sampling interval 25.06.-16.07.13 at site CBi. The potential source areas and the mineralogy of the samples are given in the subfigures a-b. The dust storm event is indicated in subfigure c.

In Fig. 12 a typical late-summer situation is illustrated. At least five separate dust events could be identified (Fig. 12f-j) out of which three occurred during the sampling interval of the site Iwik and two during the sampling interval of the site CBi. One of these dust storms occurring during the sampling interval of site CBi lasted for two days (07-08.08.2014), while all other dust storms lasted for only one day. As a result, three back trajectories could be drawn for each site and each height. The low-level back trajectories ending at site CBi run offshore. The low-level back trajectories ending at site Iwik pass through the major **PSA 2**. The high-level back trajectories pass through the major **PSA 2**, **3** and **4** (Scheuvens et al., 2013). Dust deposited in the continental traps was characterized by the presence of calcite and the absence of chlorite and kaolinite. Therefore, the source area of the dust was most likely in the Western Sahara where soils rich in calcite but poor in chlorite and kaolinite are located (Fig. 12a,b). Dust sampled with the oceanic traps during this sampling interval was characterized by the absence of chlorite and kaolinite and by the presence of a high percentage of zeolite (22 %) (Fig. 8c). Therefore, a possible source area may have been extrusive volcanic rocks of the northern Taoudeni Basin (Fig. 12c) and the Fezzan uplift (Fig. 12e). Ferryglaucophane may have been sourced by the Pharusian belt (Fig. 12d).

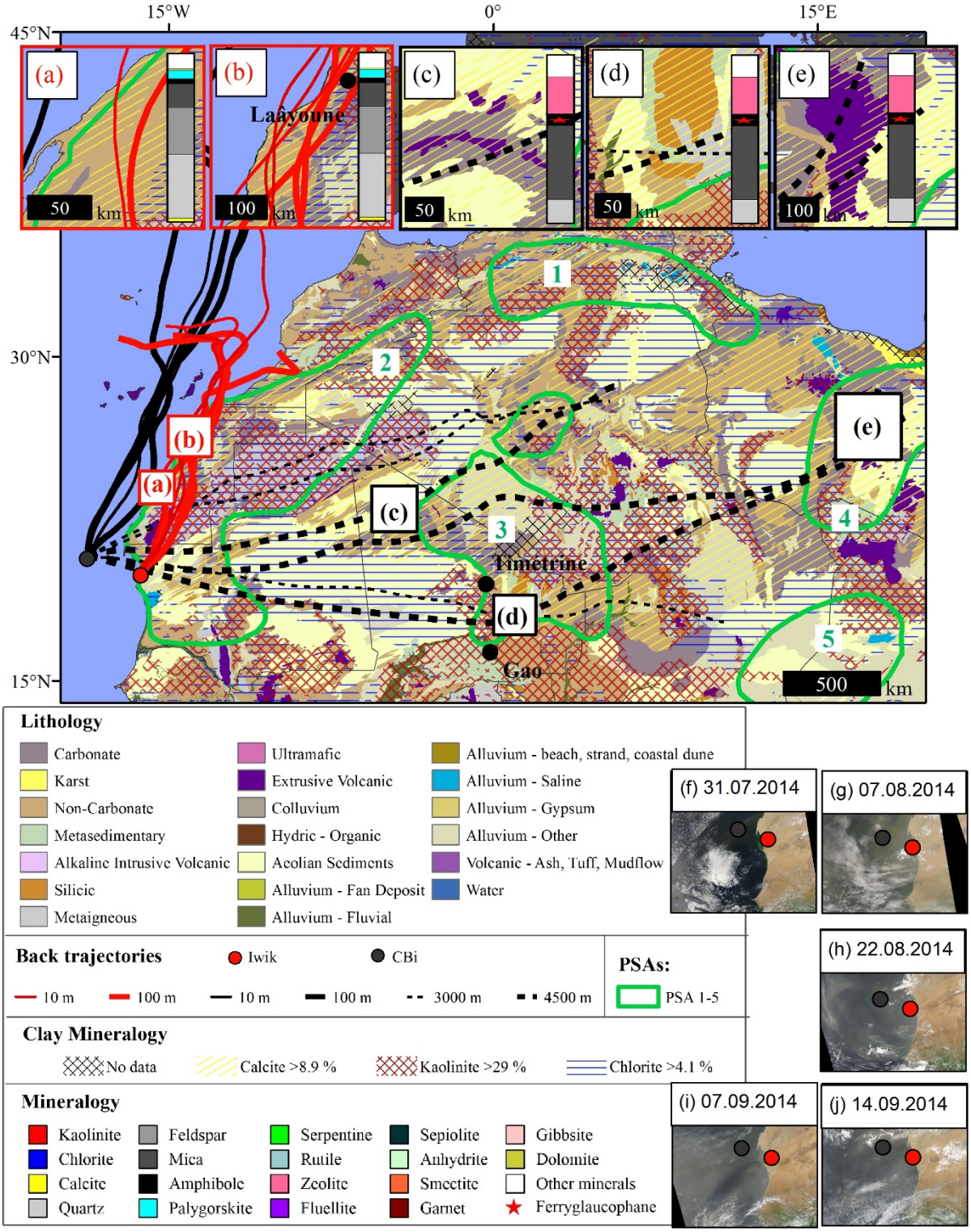

Figure 12: High- (4500 m) and low-level (10 m) four-day back trajectories of dust events ending during the sampling interval 15.08.-15.09.14 at site Iwik and during the sampling interval 01.08.-21.08.14 at site CBi. The potential source areas and the mineralogy of the samples are given in the subfigures a-c. The dust storm events are indicated in subfigures e-i.

In Fig. 13a-d the mean wind vectors and speed are presented for chosen dust storm events. The individual dust source areas that were identified using the back trajectory of the day with the dust storm as shown in Fig. 9-12 are further displayed in Fig. 13a-d. As can be clearly seen in the subfigures, the mean wind velocities were

anomalously large in the chosen dust source areas which enabled dust emission. During winter, six hourly mean wind velocities were larger than 7 ms^{-1} in the chosen dust source areas (Fig. 13a-b). During summer 2013, six hourly mean wind velocities were larger than 6 ms^{-1} in the chosen dust source area (Fig. 13c). During summer 2014 extremely high mean wind velocities were encountered near the study sites and in the proposed dust source area (Fig 13d).

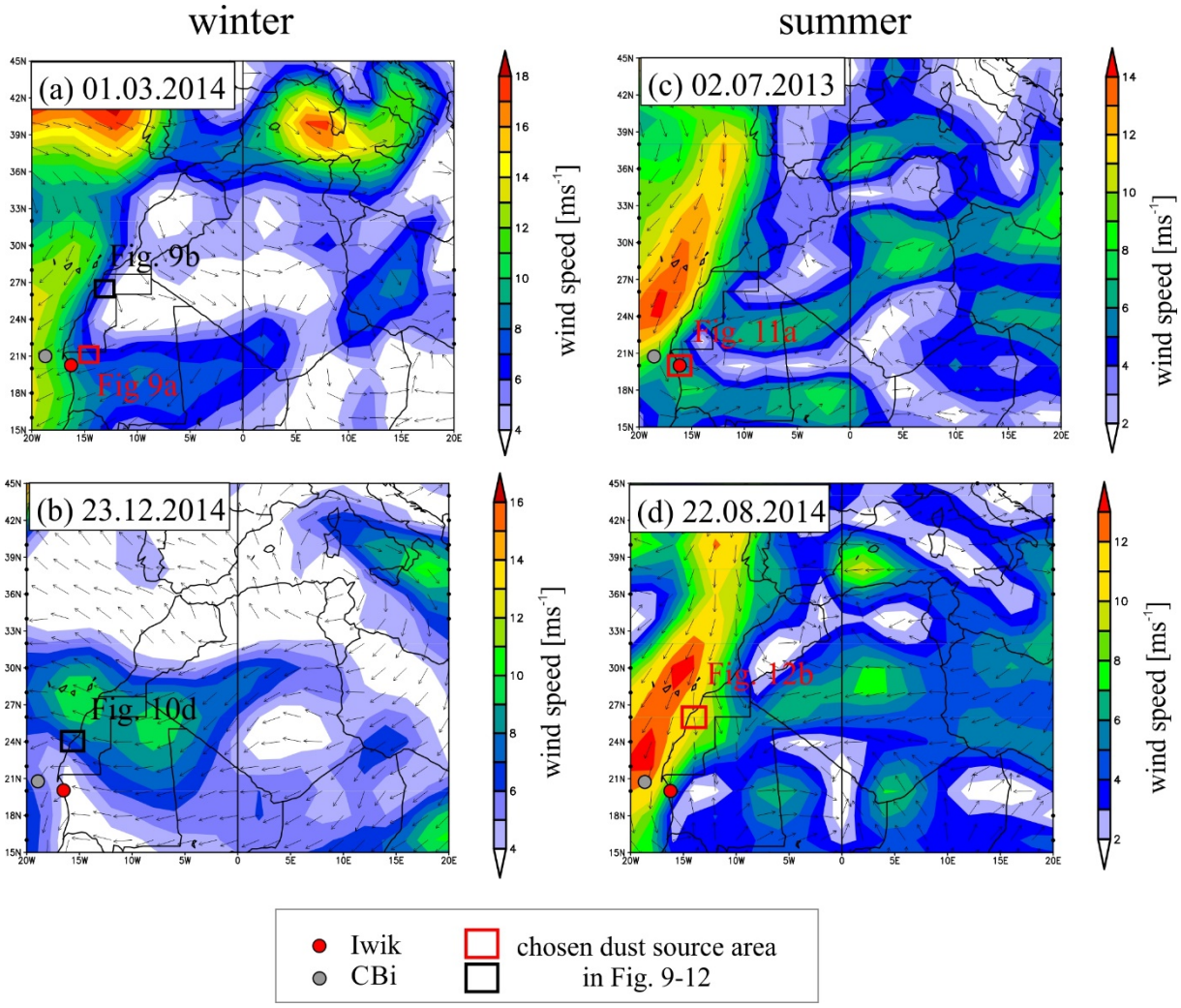

Figure 13: Six hourly composite mean wind vectors and speed at 1000 mb for selected days including a dust storm event during winter (a) – (b) and summer (c) – (d). The dust source area that was identified for the individual dust storm event using the back trajectory of the day with the dust storm is further displayed.

4. Discussion

4.1 Comparison of dust collected on land and in the ocean

4.1.1 Dust concentrations

An annual average dust concentration (total suspended particles) of ~214 μgm^{-3} and 275 μgm^{-3} was estimated for all dust samples of the year 2013 and 2014 respectively regarding the site Iwik (Table 5). These estimates were larger than what has been measured for background dust concentrations (total suspended particles) in Morocco which were in the order of 100 μgm^{-3} during spring 2006 (Kandler et al., 2009). However, in Morocco dust was collected at a larger height of 4 m and haze-periods and dust-storms were excluded from the average value. The horizontal dust fluxes at site Iwik correlated positively to wind speed (Fig. 7b) and decreased with collection height (not shown). This underscores the proximity of this continental site to the dust emission source.

At the distal oceanic site CB, the annual average dust deposition flux was ~ 45 $mgm^{-2}d^{-1}$ (2013) (Table 5). The dust flux was slightly larger than the average annual dust flux observed at site CB between 1988 and 2012 with ~ 30 $mgm^{-2}d^{-1}$ (Fischer et al., 2016). The slightly larger dust fluxes may have been caused by the anomalously high frequency in dust storm events as observed on satellite images occurring during the studied time period (not shown). The observed general decrease in the dust flux from the sites CBi and CB can be explained via the increase in the distance to the source area. Decreased dust deposition fluxes offshore NW Africa with increasing distance from the African coast were also observed by Bory and Newton (2000) analysing the lithogenic fluxes in marine sediment traps.

The average horizontal fluxes at site Iwik were ~ 1000 times larger with ~ 100000 $mgm^{-2}d^{-1}$ (Table 5) due to the different sampling technique. The MWAC samplers do not measure deposition fluxes but foremost dust concentrations. Only 1% or less drops out of a moving dust cloud within five minutes, hence, the horizontal dust flux is at least ~100 times higher than the dust deposition flux (Goossens, 2008). The fact that the dust fluxes decreased with height (not shown) further complicated a comparison between the sites due to the different sampling heights of the dust collectors (2.90 m at Iwik, versus traps in the water). Therefore, the fluxes between the site Iwik and the offshore sediment trap moorings cannot be compared.

4.1.2 Dust transport

The measured grain-size distributions for dust trapped at 2.90 m on land at site Iwik and for dust settling in the ocean were predominantly unimodal (Fig. 6). Unimodal grain-size distributions are typical for wind-blown sediments (Pye, 1995). Unimodal grain-size distributions were also measured for dust deposited in a vertical dust sampler in M'Bour (Skonieczny et al., 2011), dust sampled on ship vessels (Stuut et al., 2005) and in other sediment trap samples offshore NW Africa (Ratmeyer et al., 1999b;Van der Does et al., 2016a;Friese et al., 2016).

The measured annual average modal grain size at site Iwik was 48 µm (Table 5). The obtained average annual modal grain size was close to the coarse mode of 44 µm observed by Gillies et al. (1996) for dust trapped at a height of 10 m during spring in Fakarbé (Mali) which is located about 700 km southeast of Iwik. Gillies et al. (1996) conclude that the coarse mode in the dust samples points to locally-derived dust. Based on this observation, we argue that also the dust trapped near Iwik was most likely generally of regional instead of long-distance

provenance. The distance to the main source area may be, however, not in the direct surrounding of the dust collector since dust sampled with MWAC samplers in the vicinity of barchan dunes of the Bodélé depression at 2.4 m height is characterized by a larger modal particle size of ~ 100 µm (Chappell et al., 2008). The annual average modal and maximum particle size gradually decreased from the on-land site Iwik, to the proximal oceanic site CBi and the distal oceanic site CB (Table 5, Fig. 6a). This decrease in particle size between the stations CB and CBi was observed before and was attributed to the preferred gravitational settling of coarse particles during dust transport (Friese et al., 2016). Moreover, many studies have confirmed a downwind fining of the terrigenous fraction of surface sediments offshore NW Africa (Koopmann, 1981;Holz et al., 2004;Fütterer, 1980;Radczewski, 1939;Lange, 1975), and it is intuitively logical.

Bimodal grain-size distributions typically indicate the sampling of different dust sources (Stuut et al. (2009) and references therein). The three samples of the Iwik time series that were characterized by an additional small peak in the grain-size distribution around ~ 16 µm were sampled during sampling intervals of anomalously high wind velocity. The back-trajectories of one of these samples pointed towards a proximal and more distal dust source (Fig. 12a,b). Therefore, it may be possible that wind velocities were high enough during the sampling interval to inject dust to higher altitude and transport it from more distant sources (Fig. 12b) to the sampling site resulting in the small peak in the grain-size distributions. This interpretation is further supported by the reanalysis wind vector maps showing anomalously high wind velocities between the site Iwik and the proposed distant source area enabling dust emission and transport of dust particles from the more distant source to the site Iwik (Fig. 13d). On the other hand, microscopic examination prior to particle-size analyses of the Iwik samples revealed that the samples included many aggregates (Fig. 5d). Hence, locally derived aggregates may have been sampled during periods of high wind velocities. These aggregates may have been dispersed in the demineralized water during the measurement of the laser resulting in the observed additional fine peak at ~16 µm. Further, precipitation was encountered according to the TRMM data during the sampling interval of two of these three samples. Therefore, a further explanation for the bimodal grain-size distributions may be the deposition of finer dust particles from higher altitude of the SAL due to precipitation. The rain droplets may have evaporated during their fall releasing the dust particles at lower altitudes which can then be sampled with the MWAC sampler. However, we also observed some remnants of water in the bottles and therefore wet deposition into the bottles may have also occurred. During summer, frequent rainfall resulted in a decrease of the modal particle size of deposited Saharan dust at the site Iwik (Fig. 7c). This observation may also be explained by the deposition of finer dust particles from higher altitude of the SAL due to precipitation. One winter and one summer sample of the oceanic samples that were characterized by bimodal grain-size distributions have several proposed dust source areas each (Fig. 10, 12). Thus, the sampling of long- as well as short-travelled dust may have resulted in a bimodal grain-size distribution.

Both at the onshore sampling site Iwik and at the offshore sampling site CBi a clear seasonal trend in the particle sizes of deposited dust could be observed with generally coarser modal particle sizes during summer (Fig. 6b,c). Generally coarser summer modal particle sizes of deposited dust at site CBi were observed before for a three year time series during 2003 to 2006 and related to moist convective dust storm events (Friese et al., 2016). The generally coarser particle sizes during summer at the site Iwik may be explained by the trade wind speed as a positive correlation between the modal grain sizes and surface wind velocities was observed (Fig. 7a). This implied that dust was predominantly transported with the trade winds from sources of a quite constant distance year-round. During dust storm events particles with a diameter of 40 to 50 µm may be transported ~ 100 km (Tsoar and Pye,

1987). The proposed source areas all fall in this range except for the winter sample of 2014-2015 (Fig. 10). The winter sample was characterized by an anomalously low modal grain size of 38 µm and particles of this size may be transported more than 100 km during dust storm events (Tsoar and Pye, 1987). Moreover, Van der Does et al. (2016a) observed how particles up to 100 µm were transported ~ 3500 km across the Atlantic Ocean. To sum up, the seasonal variability in the particle size of deposited dust at the site Iwik was mainly driven by the surface wind speed due to the predominant sampling of nearby dust sources year-round.

4.1.3 Dust mineralogical composition

In the dust sampled at Iwik the minerals quartz, feldspar, mica, amphibole, palygorskite, chlorite, calcite, dolomite, gibbsite, rutile and serpentine were present (Fig. 8a). The observed occurrence of the minerals quartz, feldspar, mica, chlorite and calcite has also been described for the bulk size fraction of soil samples and dust samples collected in Mauritania (Schütz and Sebert, 1987). Palygorskite, mica and chlorite have also been detected by Skonieczny et al. (2013) in the PM_{30} size fraction of a three-year time series of dust deposition at M'Bour, Senegal, more than 500km south of Iwik, Mauritania. Smectite and kaolinite, which were absent in the Iwik samples, were the dominant minerals of the dust sampled at M'Bour (Skonieczny et al., 2013). Smectite and kaolinite are considered as indicative for wet tropical soils and their relative abundance in soils increases southwards along the northwest African coast (Lange, 1982;Biscaye, 1964). We argue that the mineralogical differences between the two sites are explained by the >500 km distance between Iwik and M'Bour and the fact that the latter station is surrounded by tropical soils. Gibbsite, rutile and serpentine have not been reported in any continental dust study so far and thus seem to be indicative for locally-derived dust (Fig. 9a, Fig. 11a).

The dust sampled at the proximal marine site CBi contained the minerals quartz, feldspar, mica, amphibole, palygorskite, chlorite, zeolite, kaolinite, smectite, sepiolite, rutile, garnet, anhydrite and fluellite (Fig. 8a). The first seven of these minerals were also found in the clay and/or silt and sand fraction of Saharan dust sampled during ship cruises parallel to the coast about 70 km off Cape Blanc (Chester et al., 1971) and perpendicular to the coast about 80 to 180 km off Cape Blanc (Chester and Johnson, 1971b). Analogous to the samples of this study, the PM_{20} fraction of surface sediments of the piston cores RC05-57, RC05-60 and A180-44 also feature zeolites and the surface sediments of core RCRC05-57 also traces of pyrophyllite (sepiolite belongs to the pyrophyllite group) (Biscaye, 1964). Further, rutile was also present in the silt and sand fraction of Saharan dust sampled perpendicular to the coast on the research vessel (Chester and Johnson, 1971b). Palygorskite was found in the clay fraction of the surface sediment of sediment core GIK12329 (19° 22' N, 19°56' W) offshore Cape Blanc and is considered a characteristic mineral of Saharan dust (Lange, 1975). The observed annual average C/K ratio (C/K=4) recorded for the bulk size fraction of the trap samples was larger than the C/K ratio (C/K=0.3-1) recorded in the clay fraction of surface sediment samples offshore Cape Blanc by Lange (1982). The disagreement may be due to the generally larger percentage of kaolinite in the clay fraction compared to the silt fraction (Journet et al., 2014).

The dust samples of the site Iwik were further characterized by a dominance in quartz and feldspar (Fig. 8a). A dominance in quartz has also been described for continental dust samples and soil samples collected in Mauritania by Schütz and Sebert (1987). More than 20 papers published XRD data of northern African dust reporting quartz as the main mineral in most dust samples (Scheuvens et al., 2013). The observed increase in micas and decrease in quartz and feldspar observed for the marine samples relative to the Iwik samples (Fig. 8a) can be explained via

the preferential gravitational settling of the larger dust minerals quartz and feldspar during transport (Delany et al., 1967;Glaccum and Prospero, 1980;Chester and Johnson, 1971b;Schütz and Sebert, 1987). A strong downwind decrease in quartz content in Saharan dust was also observed by Korte et al. (2016).

4.2 Mineralogy as a provenancing tool

In Table 7 an overview of the chosen dust source areas for the site Iwik and CBi is given together with the characteristic minerals of the samples that may be used as a tracer for the source area. In the following subsections the identification of the source areas and mineralogical tracers is described in detail.

Table 7: Overview of the chosen source areas and the tracer minerals of the individual samples together with the given characteristics of the source areas according to literature.

Sampling interval	Characteristic minerals of sample	Chosen dust source area	Bulk mineralogical composition of chosen PSA [16]	Characteristic source rocks and deposits of chosen source area
Iwik				
15.02.-15.03.14	*Rut, Serp, Cc	**PSA 2**: Reguibat Shield	C/K = 0.0–1.0 *Pal: 1-30 wt%	Metamorphic and granitic rocks [1] Serpentinites [2]
15.12.14-18.01.15	*Cc, Chl, Pal (8 wt. %)	**PSA 2:** Senegal-Mauritania Basin	C/K = 0.0–1.0 *Pal: 1-30 wt%	Chalky horizons [3]
		PSA 3: Eastern Taoudeni Basin	C/K = 0.2–0.9 *Pal:1-5 wt%	Carbonate sequences [4]
24.06.-15.07.13	*Gib	**PSA 2:** Tidra Island	C/K = 0.0–1.0 *Pal: 1-30 wt%	Gibbsite maximum offshore Cape Blanc [5]
15.08.-15.09.14	*Cc, Dol, Pal (5 wt. %)	**PSA 2:** Aaiun-Tarfaya Basin	C/K = 0.0–1.0 *Pal: 1-30 wt%	Limestone deposits [6] Outcrops near Laâyoune with dolomites [6]
CBi				
26.02.-18.03.14	*Chl, Kao (C/K = 1), Pal (11 wt. %), Flu, Anh, Sme, Ga	**PSA 2:** Aaiun-Tarfaya Basin near Boucraa	C/K = 0.0–1.0 *Pal: 1-30 wt%	Phosphate deposits [7]
16.12.14-04.01.15	*Kao (C/K = 0), Pal (1 wt. %), Zeo, Se, Sme	dike swarms and sills of northern Taoudeni Basin	-	Basalts with glass [9]
		PSA 2: Aaiun-Tarfaya Basin	C/K = 0.0–1.0 *Pal: 1-30 wt%	Palygorskite-sepiolite mafic clays [7]
		Southern Senegal-Mauritania Basin	-	Lateritic soil [8] Horizontal layers of palygorskite and sepiolite [8]
25.06.-16.07.13	*Chl, Pal (2 wt. %), Rut	**PSA 2:** Mauritanides	C/K = 0.0–1.0 *Pal: 1-30 wt%	Strongly metamorphosed rocks [10] Greenschist facies [11]
01.08.-21.08.14	*Fe-Amf, Zeo	dike swarms and sills of northern Taoudeni Basin	-	Basalts with glass [9]
		PSA 4: Fezzan uplift	C/K = 0.0–2.6 *Pal: 0 wt%	Zeolite in basaltic rocks [12,13]
		PSA 3: Pharusian belt	C/K = 0.2–0.9 *Pal:1-5 wt%	Blueschists [14] Glaucophane bearing eclogites [15]

* Amf = amphibole, Pal = palygorskite, Chl = chlorite, Cc = calcite, Dol = dolomite, Gib = gibbsite, Zeo = zeolite, Kao = kaolinite, Sme = smectite, Se = sepiolite, Rut = rutile, Serp = serpentine, Ga = garnet, Anh = anhydrite, Flu = fluellite

[1] Schofield et al. (2006) and references therein [2] Schlüter (2008) [3] Wissmann (1982) [4] Bertrand-Sarfati et al. (1991) [5] Biscaye (1964) [6] Bosse and Gwosdz (1996) [7] Moreno et al. (2006) [8] García-Romero et al. (2007) [9] Verati et al. (2005) [10] Villeneuve (2005), [11] Dallmeyer and Lécorché (2012) [12] Abdel-Karim et al. (2013) [13] Cvetković et al. (2010) [14] Caby (2014), [15] Caby et al., (2008) [16] Scheuvens et al. (2013)

4.2.1 Dust collected on land

The variability of the mineralogical composition of dust sampled at site Iwik could be related to the synoptic scale change in the surface trade wind direction. However, meteorological data from nearby sites like e.g., Nouadhibou demonstrate that local effects like the topography exert a strong influence on observed wind directions at ground level. (Fig. 2). The back trajectories indicate that the dust sources for the dust collected in Iwik during winter were located NE and E of the sampling site (Fig. 9a, Fig.10a,b), while those during summer were located W (within the PNBA) and NNE of the sampling site (Fig. 11a, Fig. 12a,b). This is in accordance with a change in the dominant local surface trade wind direction from NE in winter to NNE in summer (Fig. 2) and is also reflected in the clay-mineralogical composition of the samples.

Generally, there is not much variability in the clay-mineralogical composition of the Iwik samples. The back trajectories for the winter sample of 2014 indicate that the material was blown from the southwestern Reguibat Shield (**PSA 2)** (Fig. 9a). The lack of palygorskite in this sample does not fit to the proposed bulk palygorskite content (1-30 %) of **PSA 2** (Scheuvens et al., 2013) (Table 7). Therefore, we argue that the sampled dust was most likely derived from a localized source of **PSA 2**.

The sample included the characteristic minerals rutile and serpentine (Table 7) which are usually a result of metamorphic processes (Deer et al., 1992). Indeed, the western Reguibat Shield is composed of metamorphic and granitic rocks (Schofield et al. (2006) and references therein) and the rocks are intruded by serpentinites (Schlüter, 2008). The sample was further characterized by the highest quartz percentage among all samples (~ 50 %) (Fig. 8b). The sand dunes of the Azefal sand sea which cover part of the southwestern Reguibat Shield might have sourced these quartz grains (Fig. 9a). The sand dunes may have been fed by outcropping carbonate deposits at the northern rim of the Taoudeni Basin via the NE-trade winds leading to anomalously high percentages of calcite in the sand dunes (Fig. 9). Thus, the sand dunes may have also sourced the calcite present in the sample (Fig. 8b).

The winter sample of 2014-2015 was suggested to be sourced from sediments of the northern Senegal-Mauritania Basin (**PSA 2**) (Fig. 10a) and the eastern rim of the Taoudeni Basin (**PSA 3**) (Fig 10b). The palygorskite content of the sample (8 %) fits to the proposed bulk palygorskite content of **PSA 2** (Scheuvens et al., 2013) (Table 7). This may point to several externally mixed sources of **PSA 2** during transport.

The sample was further characterized by calcite and chlorite (Table 7). The sediments in the northern Senegal-Mauritania Basin (Fig. 10a) comprise Quaternary chalky horizons (Wissmann, 1982) which may have sourced the calcite. More likely, calcite may have been derived from the Mesozoic carbonate sequences cropping out in the eastern rim of the Taoudeni Basin (Bertrand-Sarfati et al., 1991) (Fig. 10b). A source area lying at the Algerian/Mali border was also suggested for a chlorite and calcite bearing dust sample collected on the Canary Islands (Alastuey et al., 2005). The winter dust sample trapped at site Iwik was further characterized by the lowest feldspar percentage (~ 5 %), highest mica percentage (~ 40 %) (Fig. 8b) and lowest modal grain size (~ 38 µm) among all Iwik dust samples analysed for mineralogy. The Stokes terminal settling velocity is smaller for platy particles than for spherical particles of similar diameter (Santamarina and Cho, 2004). Therefore, a long-distance transport of dust from the eastern Taoudeni Basin to Iwik may have resulted in a depletion in spherical quartz particles (Fig. 5a,b,c) and an enrichment in platy mica particles (Fig. 5b).

The summer sample of 2013 was proposed to be sourced from the near-by northern Tidra Island (**PSA 2**) (Fig. 11a). Again, the absence of the mineral palygorskite is noteworthy which may point to the sampling of a localized dust source.

The sample was further characterized by the mineral gibbsite (Table 7). The northern Tidra Island is famous for the local occurrence of west Africa's northernmost mangroves (Proske et al., 2008) which grow in humid and warm climates. Humid and warm conditions are also beneficial for the formation of gibbsite which forms through tropical weathering (Deer et al., 1992). Therefore, we argue that the soils of Tidra Island supplied the gibbsite found in the sample. A localized small gibbsite maximum was outlined for the surface sediments offshore Cape Blanc (Biscaye, 1964) which further supports the view that gibbsite is supplied from a local source. The sample was further characterized by anomalously large moderately spherical quartz grains (Fig. 5c) emphasizing a short travel distance of the dust.

The summer sample of 2014 was most likely sourced by sediments of the Western Sahara (**PSA 2**) (Fig. 12a,b). The palygorskite content of the sample (5 %) matches with the proposed bulk palygorskite content of **PSA 2** (Scheuvens et al., 2013) (Table 7). Hence, dust may have been supplied from several dust sources of **PSA 2** which were mixed during transport.

The sample was further characterized by calcite and dolomite (Table 7). Sediments outcropping in the Western Sahara are composed of Tertiary sediments (Wissmann, 1982) with limestone deposits (Bosse and Gwosdz, 1996) that may explain the calcite found in the sample (Fig. 12a). Upper cretaceous outcrops in the Aaiun-Tarfaya Basin near Laâyoune comprise dolomites (Bosse and Gwosdz, 1996) and could have sourced the dolomite found in the sample (Fig. 12b). A further evidence for dolomite-bearing dust transport from the Aaiun-Tarfaya Basin is a local dolomite maximum outlined for the surface sediments offshore the Western Sahara (Johnson, 1979). A Saharan dust sample trapped in NE Spain also contained dolomite and calcite and was related to a source area lying in the Western Sahara (Avila et al., 1997).

4.2.2 Dust collected at the marine sites

The seasonal contrast in the dust transport patterns (high-level SAL vs. low-level Trades) potentially leaded to strongly deviating dust sources for the material deposited in the marine trap samples. During winter, the back trajectories indicated that the potential dust source areas were located NE of the sampling site (Fig. 9b, Fig. 10c,d,e), while those during summer were located NE, E and SE of the sampling site (Fig. 11b, Fig.12c,d,e). This large variability in wind patterns can clearly be recognized in the clay-mineralogical compositions of the samples throughout the seasons.

Considering the much larger catchment area of the traps, several dust sources may have been sampled with the traps. As a result, the composition of the analyzed samples fit well to the bulk composition of the chosen **PSA**. The back trajectories indicate that the winter sample of 2014 originated from the shoreline of the Western Sahara (**PSA 2**) (Fig. 9b). The observed C/K ratio (C/K=1) and the palygorskite content (11 %) are in agreement with the bulk compositional C/K ratio (C/K=0-1) and palygorskite content of **PSA 2** (Scheuvens et al., 2013) (Table 7).

The sample was further characterized by the presence of garnet, fluellite and anhydrite (Table 7). The characteristic occurrence of garnet together with the highest quartz content (33 %, Fig. 8b) among all CBi samples confirms a

short transport distance of the trapped dust. The mineral fluellite which is a weathering product of phosphate may have been derived from outcropping phosphate deposits near the Bucraa phosphate mine (Moreno et al., 2006) (Fig. 9b). Anhydrite could originate from evaporites along the coast.

The back trajectories of the winter sample of 2014 to 2015 lead to the Reguibat Shield (**PSA 2) (**Fig. 10c), the coastal Western Sahara (**PSA 2)** (Fig. 10d) and the southern Senegal-Mauritania Basin (Fig. 10e). The observed C/K ratio (C/K=0) and palygorskite content (1 %) fall within the ranges of these minerals in **PSA 2** (Scheuvens et al., 2013) (Table 7). Therefore, the **PSA 2** may have been the dominant source area of the sampled dust.
The sample was further characterized by the minerals zeolite, kaolinite, sepiolite and smectite (Table 7). Zeolites are formed from volcanic glass and tuff and form well-developed crystals in basalts (Deer et al., 1992). Therefore, the source area of the zeolites may have been outcropping volcanic rocks in the northern Taoudeni Basin (Fig. 10c). These rocks belong to mafic dikes and sills which are commonly basalts with dotted patches of glass (Verati et al., 2005). An additional indication for a distant dust source may be the lowest quartz content (4 %) among all samples (Fig. 8b). Palygorskite-sepiolite mafic clays were found in soil samples of the Western Sahara (Moreno et al., 2006) which may supports a Western Saharan source (Fig. 10d).
Sepiolite belongs to the pyrophyllites which is a mineral that also may be considered indicative of tropical weathering (Moore and Reynolds, 1989). Moreover, kaolinite is usually considered indicative of tropical weathering and the laterites of the southern Sahara and Sahel (Lange, 1975;Biscaye, 1964;Lange, 1982). Outcrops of quaternary laterites as well as outcrops of lower Eocene horizontal layers of palygorskite and sepiolite were described near Thiès in Senegal (García-Romero et al., 2007). Therefore, the kaolinite-rich soils and outcrops in the southern Senegal-Mauritania basin near Thiès (Fig. 10e) may have served the kaolinite, sepiolite and palygorskite found in the sample.
Another explanation for the presence of kaolinite and smectite in the sample may be the transport of these minerals from southern latitudes via the poleward-flowing undercurrent to the trap site CBi (Fig. 1). Kaolinite and smectite were found in the clay fraction of the surface sediments off Senegal (Nizou et al., 2011) and may have been brought into the ocean by the Senegal River, and redistributed by ocean currents (Biscaye, 1964). The season of high Senegal River sediment supply is between July to October/November (Gac and Kane, 1986). Assuming a mean speed of ~10 cm/s of the undercurrent (Mittelstaedt, 1991), it may take about two months for the particles to travel a distance of ~500 km to the trap site CBi. This time delay might explain the observed occurrence of these minerals in the trap samples during winter, but not during summer.

Based on the back trajectories, the summer sample of 2013 was suggested to be sourced from the Mauritanides (**PSA 2)** (Fig. 11c). This is confirmed by the palygorskite content of the sample (2 %) (Scheuvens et al., 2013) (Table 7). Outstanding minerals in this sample are chlorite and rutile (Table 7). Outcrops in the Mauritanides west of the Taoudeni Basin feature strongly metamorphosed rocks (Villeneuve, 2005) and greenschist facies (Dallmeyer and Lécorché, 2012) which may have been the source of the rutile and chlorite.

The reconstructed source area of the summer sample of 2014 was the Pharusian belt (**PSA 3)** (Fig. 12c), the extrusive volcanics of the northern Taoudeni Basin (**PSA 2)** (Fig. 12d) and the Fezzan uplift (**PSA 4**) (Fig. 12e). The lack of palygorskite in the sample does corroborate with **PSA 4** ('not detected') (Scheuvens et al., 2013) suggesting that the provenance of the dust sample may be mainly confined to **PSA 4** (Table 7).

887 The sample was further characterized by zeolite and ferryglaucophane (Table 7). The dike swarms and sills of the
888 northern Taoudeni Basin (Verati et al., 2005) (Fig. 10c, Fig. 12c) and/or the basalts of the Fezzan uplift (Fig. 12e)
889 may have sourced the zeolite. Indeed, zeolite was described as one of the main secondary minerals in the basaltic
890 rocks of the central Al-Harui Al-Abyas basalt flows (Abdel-Karim et al., 2013) and in vesicles of the east Al Haruj
891 basalts (Cvetković et al., 2010) of the Fezzan uplift. Traces of zeolite were also detected in the Iwik sample during
892 this sampling interval. It may be that the zeolite dropped out of the high-altitude dust cloud and was subsequently
893 transported via the surface trade winds to the continental trap site. The presence of ferryglaucophane and the
894 absence of feldspar and chorite in the sample indicates highly metamorphous outcrops constituting the dust source.
895 Therefore, the sample may have been additionally sourced by the Pharusian belt (Fig. 12c) because blueschists
896 were observed in Timétrine (Caby, 2014) and glaucophane bearing eclogites in the Gourma fold and thrust belt
897 north of Gao (Caby et al., 2008). The sample was further characterized by the highest mica content (44 %) among
898 all samples (Fig. 8c) supporting a large dust transport distance.

899

900

5. Summary and conclusions

The fluxes, grain-size distributions and the mineral assemblages of the continental trap samples and oceanic sediment trap samples were well comparable to the characteristics of Saharan dust reported for the region. The following main findings were made:

- A clear seasonal variability in the particle size of mineral dust deposited on land could be observed with generally coarser modal grain sizes during summer compared to winter. The modal particle sizes could be related to the trade wind speed.
- dust deposited on the continent was predominantly transported from near-by local sources (Mauritania, Western Sahara and Mali), while dust deposited in the marine traps was transported from proximal (Mauritania, Western Sahara and Mali) and distal sources (Senegal and Libya).
- Some rare characteristic minerals (e.g. ferryglaucophane, rutile, serpentine) could be related to local outcrops in NW Africa.

To conclude, the particle size and mineralogy of Saharan dust recorded in continental climate archives should be interpreted differently with respect to paleo-environmental conditions compared to marine climate archives; the on-land archive seems to reflect a much more local signal as compared to the regional signal that is recorded in the marine sediments. Given the relationship between particle size and wind strength, we suggest that the particle size in the continental archive in NW Africa may indicate the paleo-wind strength of the trade winds. This is an intuitively logical conclusion, but it has not been demonstrated before so clearly. It should be kept in mind, however, that the wind in the sampling location might differ from the wind in the source region if the source region is further away. Moreover, the sizes of dust particles present in the source region will influence the grain sizes of deposited dust.

6. Appendices

A1 Satellite RGB images

In Fig. A1-4 satellite RGB true colour images are shown of the identified dust storms occurring during the sampling interval of the samples analysed for dust provenance. On 31 July 2014 only few dust can be observed which overlies the sampling location CBi (Fig. A2). This fits to the observed minor percentage of the mineral ferryglaucophane (7 %) in the sample which was suggested to be sourced on 31 July 2014 from PSA 3. Zeolite, which was more abundant (22 %) in the dust sample, was therefore most likely derived from PSA 4 due to the major dust storm event occurring on 7 August 2014 (Fig. A3).

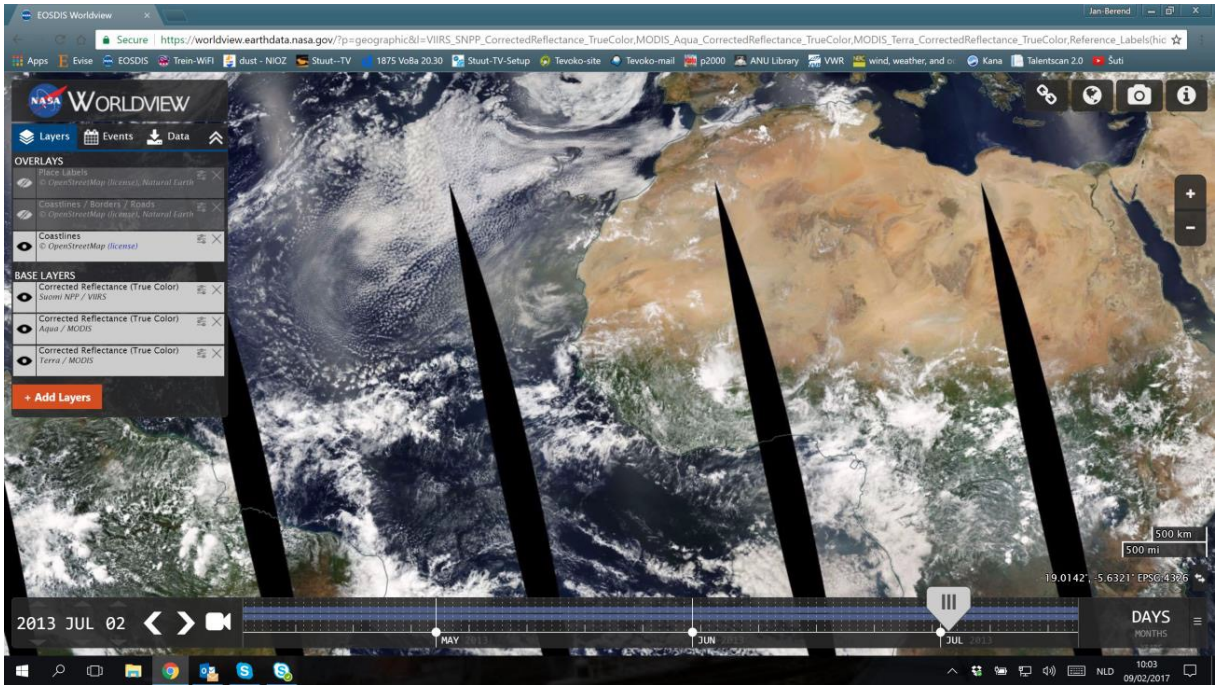

Figure A1: Dust storm on 02 July 2013.

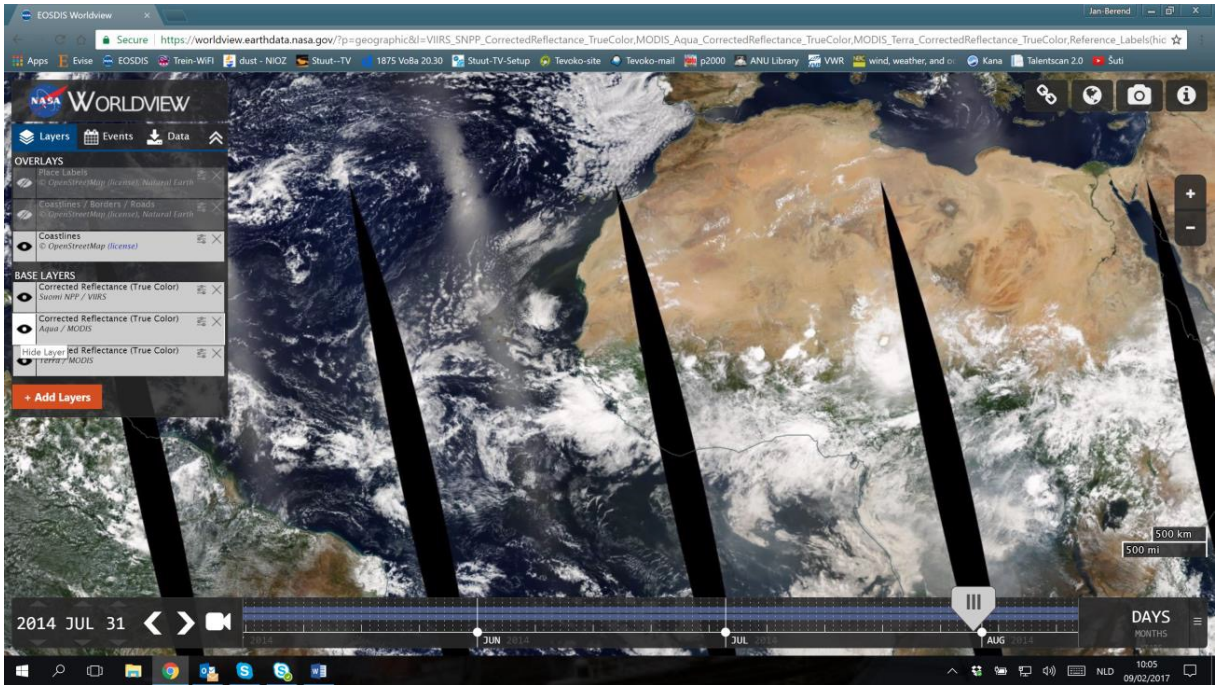

948

949 **Figure A2: Dust storm on 31 July 2014.**

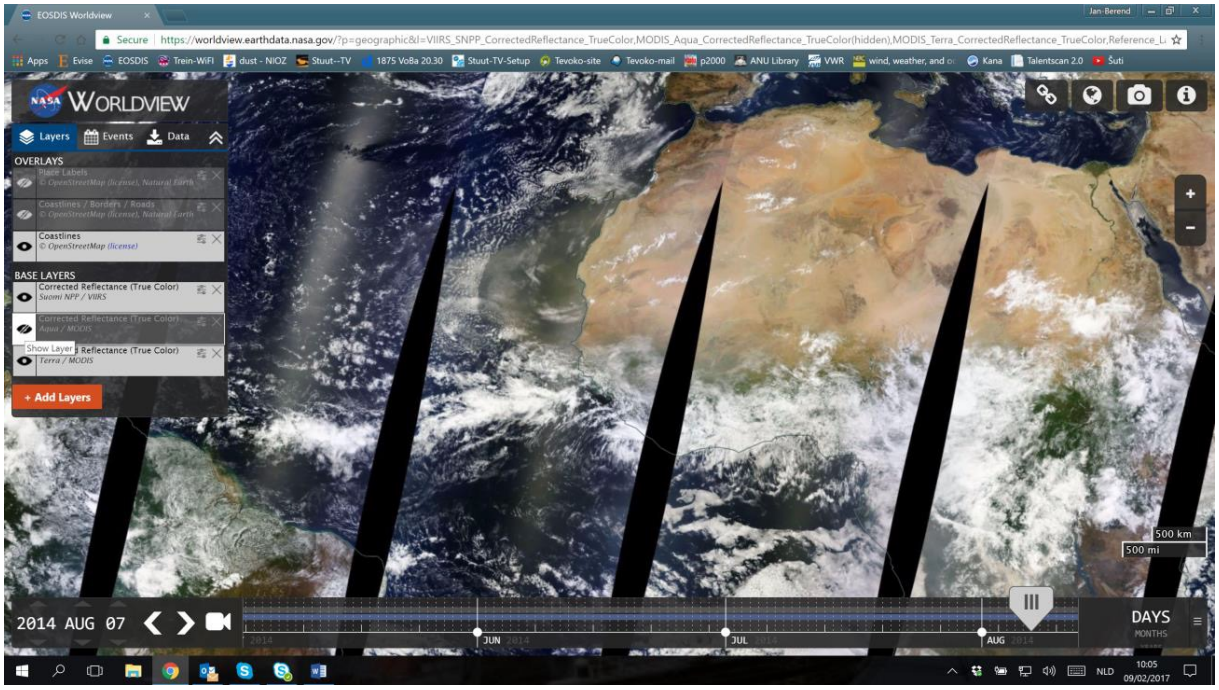

950

951 **Figure A3: Dust storm on 07 August 2014.**

952

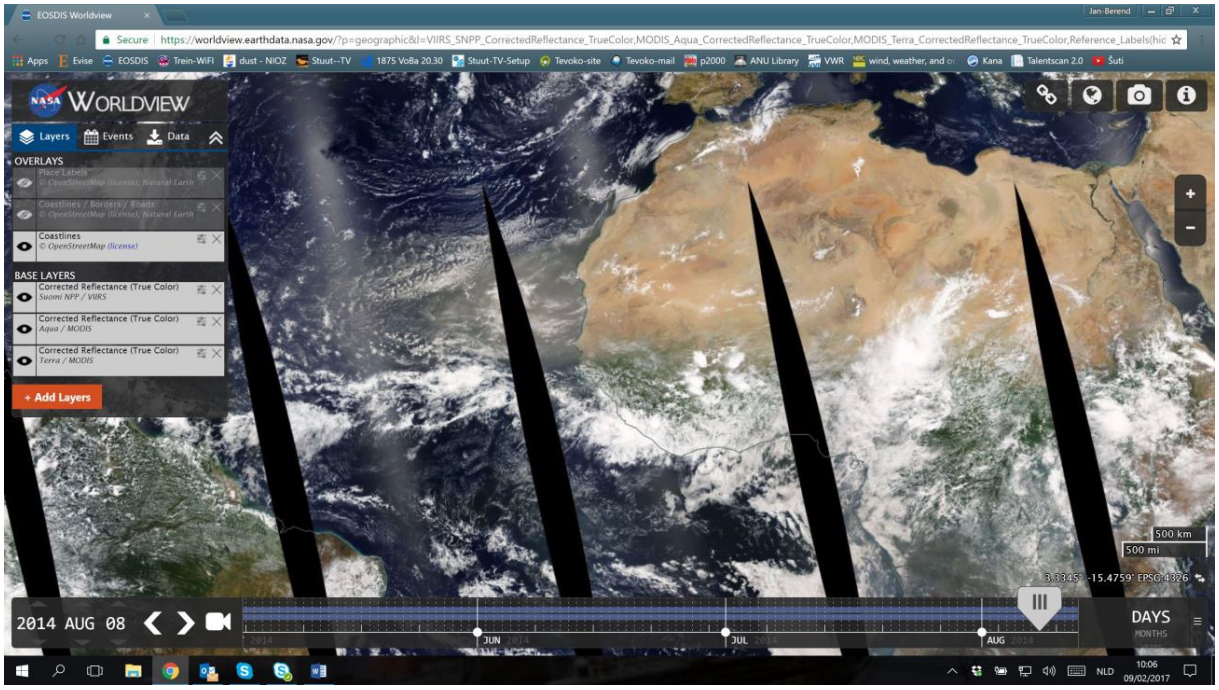

Figure A4: Dust storm on 08 August 2014.

A2 Four day back-trajectories

In Fig. A5-8 the four day back-trajectories are shown calculated at the heights 3000 m, 4500 m and 5500 m ending at site CBi. These high altitude back-trajectories were calculated for the identified summer days with dust storm events (shown in Fig A1-4). On the one hand, a height of 4500 m was chosen by Skonieczny et al. (2013) in a dust provenance study to represent the Saharan air layer (SAL). On the other hand, a height of 5500 m was chosen by Ratmeyer et al. (1999a) in a dust transport study to represent the SAL. Maximum wind velocities within the SAL are observed at a height of ~ 3 - 4 km in the area of the Cape Verde Islands during summer according to Carlson and Prospero (1972). Therefore, we also plotted the back-trajectories at a height of 3000 m. In order to investigate which air layer should be chosen for provenance studies, the back trajectories of the different heights were compared.

The back-trajectories deviated slightly from each other regarding their direction and length. The back-trajectories at 3000 m showed the most deviation. Further, the back-trajectories at 4500 m showed the best agreement with the source areas and the minerals in the samples. Therefore, we chose to use the trajectories at 4500 m for provenance studies according to Skonieczny et al. (2013).

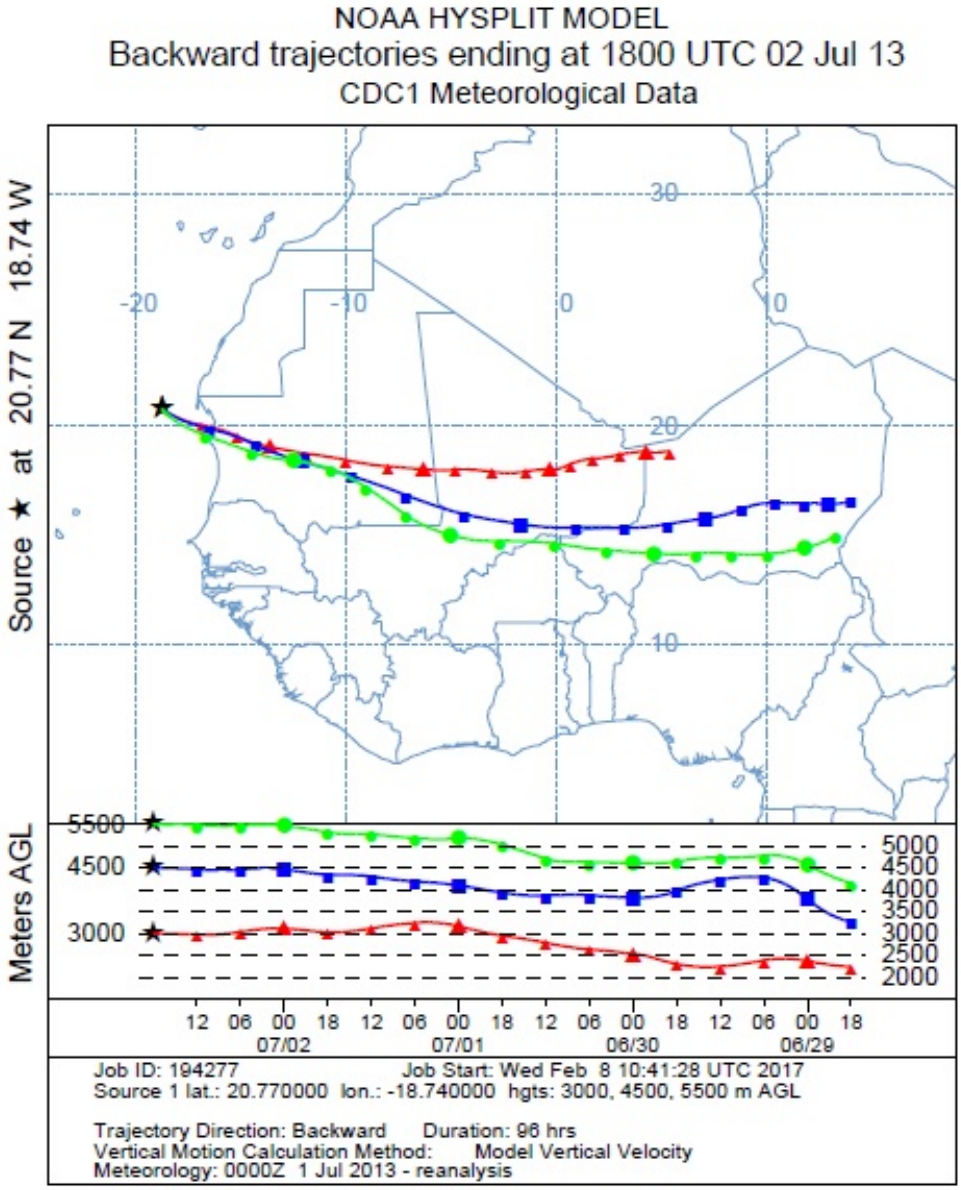

Figure A5: Four day back-trajectories at a height of 3000 m, 4500 m and 5500 m on 02 July 2013.

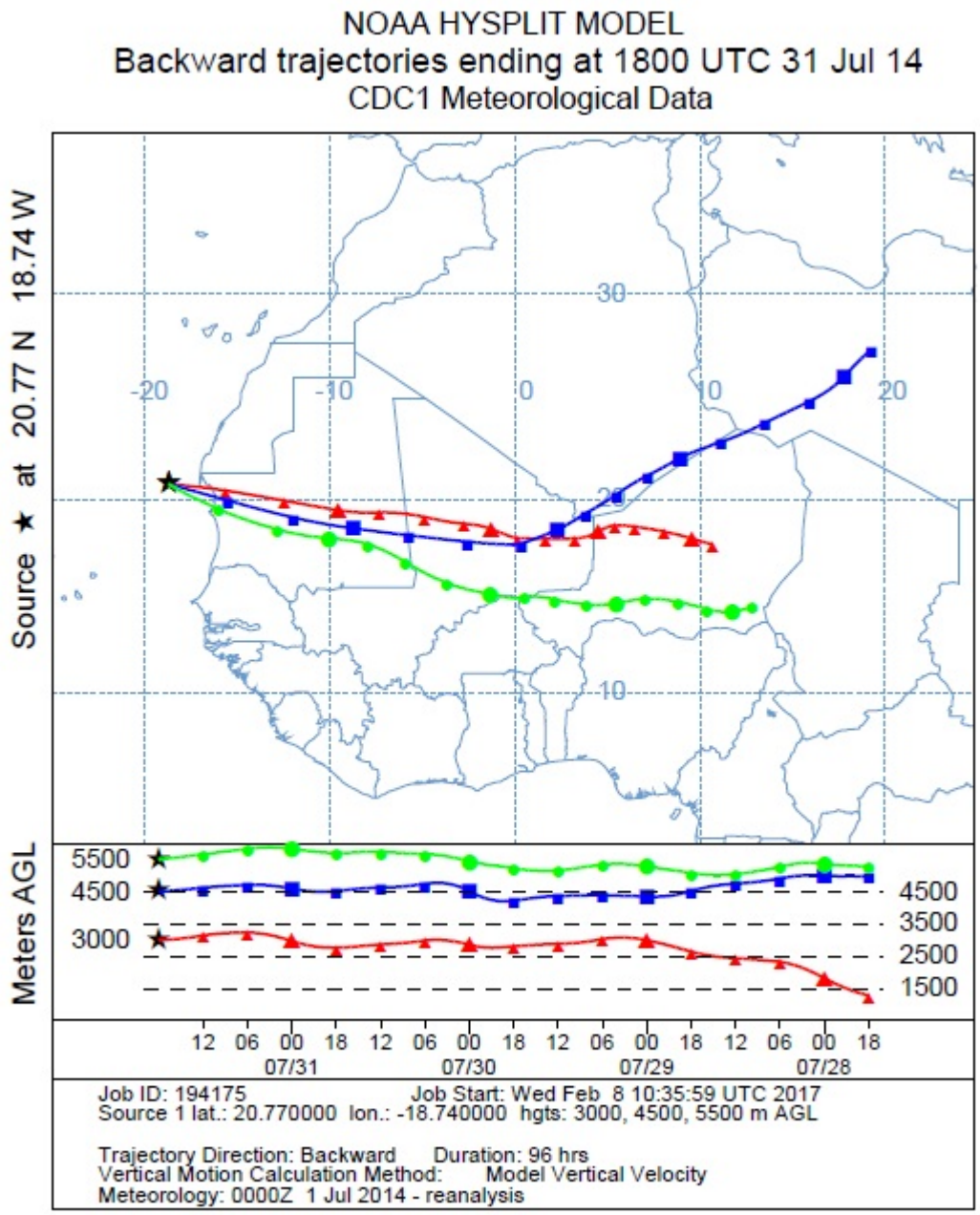

975

976 **Figure A6: Four day back-trajectories at a height of 3000 m, 4500 m and 5500 m on 31 July 2014.**

977

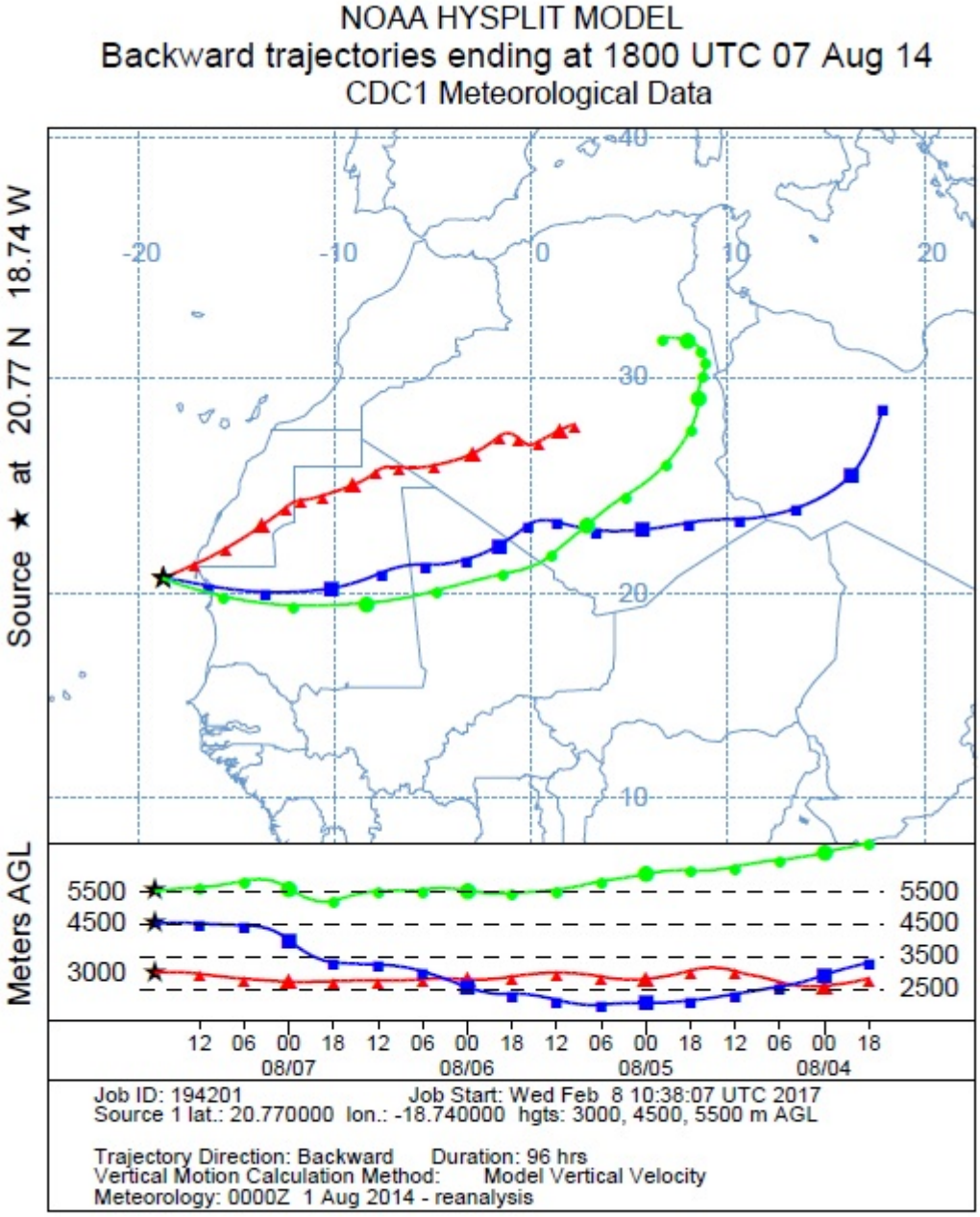

978

979 **Figure A7: Four day back-trajectories at a height of 3000 m, 4500 m and 5500 m on 07 August 2014.**

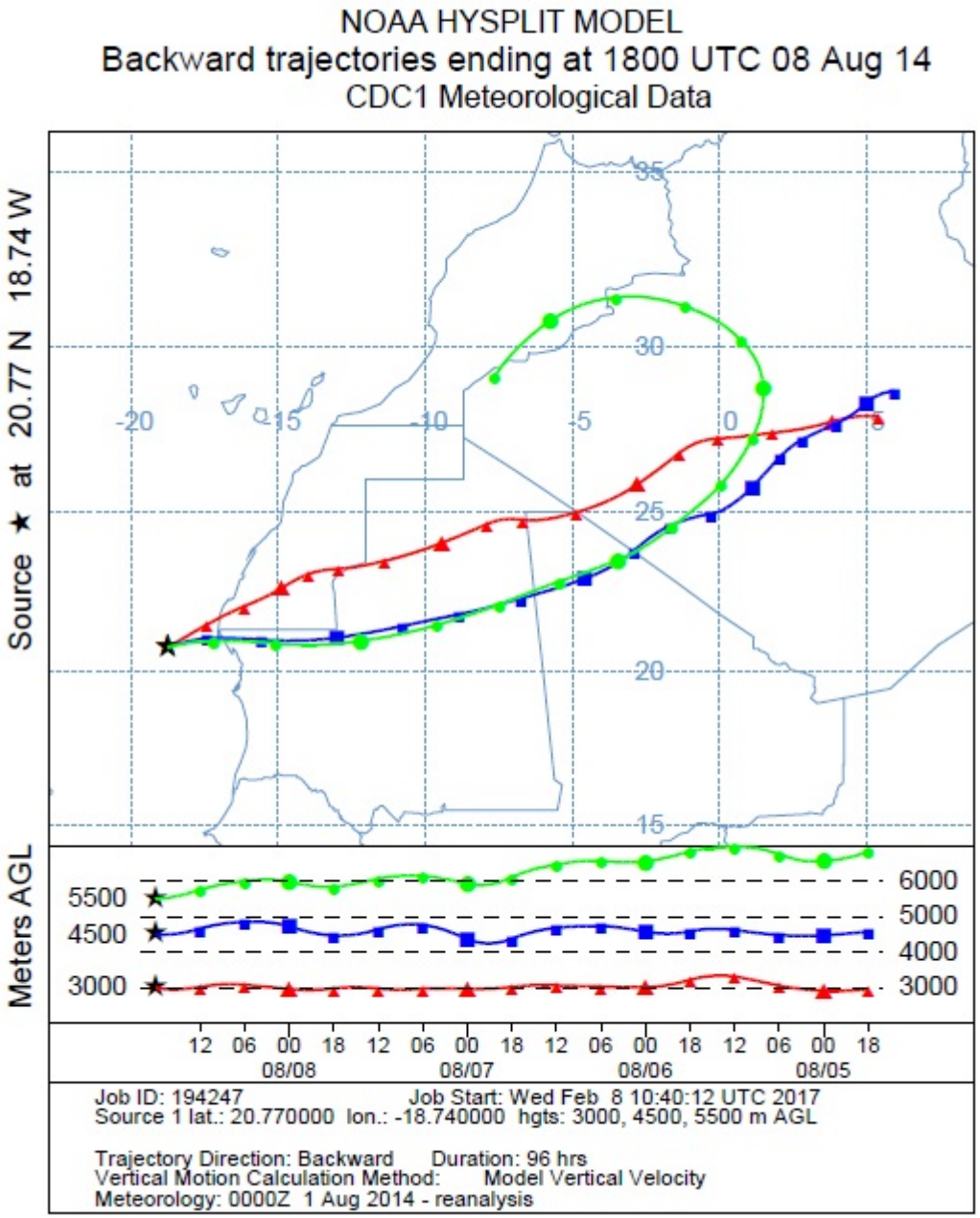

980

981 **Figure A8: Four day back-trajectories at a height of 3000 m, 4500 m and 5500 m on 08 August 2014.**

982

983

7. Supplement link

The data can be accessed on www.pangaea.de.

8. Author contribution

C. Friese carried out the particle size analysis of the sediment trap samples. H. van Hateren carried out the flux and particle size analysis of the Iwik dust samples. G. Fischer provided the sediment trap samples and supervised the flux analysis of the sediment trap samples. C. Friese prepared the samples for XRD analysis. C. Vogt carried out the XRD analysis and was involved in the discussion of the results. J.-B. Stuut managed the projects through which dust-collecting buoy 'Carmen' was constructed and deployed, supervised the particle-size analysis and the writing of the manuscript. C. Friese prepared the manuscript with contributions from all co-authors.

9. Competing interests

The authors declare that they have no conflict of interest.

10. Acknowledgements

We thank the captains, crews and scientific teams of the research cruises with RV Poseidon in 2013 (POS445), RV Poseidon in 2014 (POS464) and RV Poseidon in 2015 (POS481), during which the sediment traps were deployed and received. Further, we thank Marco Klann for preparing and splitting the sediment trap samples. Jan-Berend Stuut acknowledges funding from ERC Grant 311152 DUSTTRAFFIC. Funding is acknowledged from the German Science Foundation (DFG) through the DFG-Research Center/Cluster of Excellence 'The Ocean in the Earth System'. We further thank Prof. Dr. Dierk Hebbeln and Dr. Ute Merkel for helpful and productive scientific discussions.

11. References

Abdel-Karim, A.-A. M., Ramadan, E.-N. M., and Embashi, M. R.: Multiphase Alkaline Basalts of Central Al-Haruj Al-Abyad of Libya: Petrological and Geochemical Aspects, Journal of Geological Research, 2013, 12, 10.1155/2013/805451, 2013.

Alastuey, A., Querol, X., Castillo, S., Escudero, M., Avila, A., Cuevas, E., Torres, C., Romero, P.-M., Exposito, F., and García, O.: Characterisation of TSP and PM2. 5 at Izana and Sta. Cruz de Tenerife (Canary Islands, Spain) during a Saharan Dust Episode (July 2002), Atmospheric Environment, 39, 4715-4728, 2005.

Aston, S. R., Chester, R., Johnson, L. R., and Padgham, R. C.: Eolian dust from the lower atmosphere of the eastern Atlantic and Indian oceans, China Sea and Sea of Japan, Marine Geology, 14, 15-28, 1973.

Avila, A., Queralt-Mitjans, I., and Alarcon, M.: Mineralogical composition of African dust delivered by red rains over northeastern Spain, Journal of Geophysical Research, 102, 21977-21996, 1997.

Bertrand-Sarfati, J., Moussine-Pouchkine, A., Affaton, P., Trompette, R., and Bellion, Y.: Cover sequences of the West African craton, in: The West African orogens and circum-Atlantic correlatives, Springer, 65-82, 1991.

Biscaye, P.: Mineralogy and sedimentation of recent Deep-sea clay in the Atlantic Ocean and adjacent seas and oceans., Geol Soc Am Bull, 76, 803-832, 1965.

Biscaye, P. E.: Mineralogy and sedimentation of the deep-sea sediment fine fraction in the Atlantic Ocean and adjacent seas and oceans, Ph.D., Geology, Yale University, Michigan, 86 pp., 1964.

Bloemsma, M. R., Zabel, M., Stuut, J. B. W., Tjallingii, R., Collins, J. A., and Weltje, G. J.: Modelling the joint variability of grain size and chemical composition in sediments, Sedimentary Geology, 280, 135-148, http://dx.doi.org/10.1016/j.sedgeo.2012.04.009, 2012.

Bory, A. J. M., and Newton, P. P.: Transport of airborne lithogenic material down through the water column in two contrasting regions of the eastern subtropical North Atlantic Ocean, Global Biogeochem. Cycles, 14, 297-315, 10.1029/1999gb900098, 2000.

Bosse, H.-R., and Gwosdz, W.: Limestone and dolomite resources of Africa, Geologisches Jahrbuch Reihe D, 500, 102, 1996.

Boullier, A.-M.: The pan-African trans-Saharan belt in the Hoggar shield (Algeria, Mali, Niger): A review, in: The west African orogens and circum-Atlantic correlatives, Springer, 85-105, 1991.

Caby, R., Buscail, F., Dembele, D., Diakite, S., Sacko, S., and Bal, M.: Neoproterozoic garnet-glaucophanites and eclogites: new insights for subduction metamorphism of the Gourma fold and thrust belt (eastern Mali), Geological Society, London, Special Publications, 297, 203-216, 2008.

Caby, R.: Nature and evolution of Neoproterozoic ocean-continent transition: Evidence from the passive margin of the West African craton in NE Mali, Journal of African Earth Sciences, 91, 1-11, http://dx.doi.org/10.1016/j.jafrearsci.2013.11.004, 2014.

Caquineau, S., Gaudichet, A., Gomes, L., and Legrand, M.: Mineralogy of Saharan dust transported over northwestern tropical Atlantic Ocean in relation to source regions, Journal of Geophysical Research, 107, 4251, 2002.

1037 Carlson, T. N., and Prospero, J. M.: The Large-Scale Movement of Saharan Air Outbreaks over the Northern Equatorial
1038 Atlantic, Journal of Applied Meteorology, 11, 283-297, 1972.

1039 Chappell, A., Warren, A., O'Donoghue, A., Robinson, A., Thomas, A., and Bristow, C.: The implications for dust emission
1040 modeling of spatial and vertical variations in horizontal dust flux and particle size in the Bodélé Depression, Northern Chad,
1041 Journal of Geophysical Research: Atmospheres, 113, n/a-n/a, 10.1029/2007JD009032, 2008.

1042 Chester, R., Elderfield, H., and Griffin, J. J.: Dust transported in the North-east and South-east Trade Winds in the Atlantic
1043 Ocean, Nature, 233, 474-476, 10.1038/233474a0, 1971.

1044 Chester, R., and Johnson, L. R.: Atmospheric dusts collected off the Atlantic coasts of North Africa and the Iberian Peninsula,
1045 Marine Geology, 11, 251-260, 1971a.

1046 Chester, R., and Johnson, L. R.: Atmospheric dusts collected off the West African Coast, Nature, 229, 105-107, 1971b.

1047 Chester, R., Elderfield, H., Griffin, J., Johnson, L., and Padgham, R.: Eolian dust along the eastern margins of the Atlantic
1048 Ocean, Marine Geology, 13, 91-105, 1972.

1049 Chung, F. H.: Quantitative interpretation of X-ray diffraction patterns of mixtures. I. Matrix-flushing method for quantitative
1050 multicomponent analysis, Journal of Applied Crystallography, 7, 519-525, 1974.

1051 Cropper, T. E., Hanna, E., and Bigg, G. R.: Spatial and temporal seasonal trends in coastal upwelling off Northwest Africa,
1052 1981–2012, Deep Sea Research Part I: Oceanographic Research Papers, 86, 94-111,
1053 http://dx.doi.org/10.1016/j.dsr.2014.01.007, 2014.

1054 Cvetković, V., Toljić, M., Ammar, N. A., Rundić, L., and Trish, K. B.: Petrogenesis of the eastern part of the Al Haruj basalts
1055 (Libya), Journal of African Earth Sciences, 58, 37-50, http://dx.doi.org/10.1016/j.jafrearsci.2010.01.006, 2010.

1056 Dallmeyer, R. D., and Lécorché, J.-P.: The West African orogens and circum-Atlantic correlatives, Springer Science &
1057 Business Media, 2012.

1058 Deer, W. A., Howie, R. A., and Zussman, J.: An introduction to the rock-forming minerals, Longman Scientific & Technical,
1059 1992.

1060 Delany, A. C., Claire Delany, A., Parkin, D. W., Griffin, J. J., Goldberg, E. D., and Reimann, B. E. F.: Airborne dust collected
1061 at Barbados, Geochimica et Cosmochimica Acta, 31, 885-909, 1967.

1062 Diaz, H. F., Carlson, T. N., Prospero, J. M., and Office, E. R. L. W. M. P.: A Study of the Structure and Dynamics of the
1063 Saharan Air Layer Over the Northern Equatorial Atlantic During BOMEX, Nr. 32, Weather Modification Program Office,
1064 Environmental Research Laboratories, 1976.

1065 Diester-Haass, L., and Chamley, H.: Neogene paleoenvironment off NW Africa based on sediments from DSDP Leg 14, Journal
1066 of Sedimentary Research, 48, 1978.

1067 Dobson, M.: An account of the Harmattan, a singular African wind, Philosophical transactions of the Royal Society of London,
1068 71, 46-57, 1781.

1069 Einsele, G., Herm, D., and Schwarz, H. U.: Sea level fluctuation during the past 6000 yr at the coast of Mauritania, Quaternary
1070 Research, 4, 282-289, http://dx.doi.org/10.1016/0033-5894(74)90017-9, 1974.

El Makkrouf, A. A.: Tectonic interpretation of Jabal Eghei area and its regional application to Tibesti orogenic belt, south central Libya (S.P.L.A.J.), Journal of African Earth Sciences (and the Middle East), 7, 945-967, http://dx.doi.org/10.1016/0899-5362(88)90009-7, 1988.

Filipsson, H. L., Romero, O. E., Stuut, J.-B. W., and Donner, B.: Relationships between primary productivity and bottom-water oxygenation off northwest Africa during the last deglaciation, Journal of Quaternary Science, 26, 448-456, DOI:10.1002/jqs.1473, 2011.

Fischer, G., and Wefer, G.: Sampling, Preparation and Analysis of Marine Particulate Matter, Geoph Monog Series, 63, 391-397, 1991.

Fischer, G., and Karakas, G.: Sinking rates and ballast composition of particles in the Atlantic Ocean: implications for the organic carbon fluxes to the deep ocean, Biogeosciences, 6, 85-102, 2009.

Fischer, G., Ba, M., Dehning, K., Hefter, J., Iversen, M., Klann, M., Nowald, N., Ploug, H., Ruhland, G., and Witte, Y.: Report and preliminary results of R/V POSEIDON cruise POS445. Las Palmas–Las Palmas, 19.01. 2013–01.02. 2013, 2013.

Fischer, G., Dehning, K., Dia, A., Füssel, J., Hefter, J., Iversen, M., Klann, M., Nowald, N., Olbrich, M., and Ruhland, G.: Report and preliminary results of RV POSEIDON cruise POS464, Las Palmas (Canary Islands)-Las Palmas (Canary Islands), 03.02. 2014-18.02. 2014, 2014.

Fischer, G., Dia, A., Iversen, M., Klann, M., Nowald, N., Markussen, T., Meckel, S., Ruhland, G., Van der Jagt, H., and Waldmann, C.: Report and preliminary results of R/V POSEIDON cruise POS481, Las Palmas (Canary Islands)-Las Palmas (Canary Islands), 15.03. 2015-03.03. 2015, 2015.

Fischer, G., Romero, O., Merkel, U., Donner, B., Iversen, M., Nowald, N., Ratmeyer, V., Ruhland, G., Klann, M., and Wefer, G.: Deep ocean mass fluxes in the coastal upwelling off Mauritania from 1988 to 2012: variability on seasonal to decadal timescales, Biogeosciences Discussions, 12, 2016.

Formenti, P., Rajot, J. L., Desboeufs, K., Caquineau, S., Chevaillier, S., Nava, S., Gaudichet, A., Journet, E., Triquet, S., Alfaro, S., Chiari, M., Haywood, J., Coe, H., and Highwood, E.: Regional variability of the composition of mineral dust from western Africa: Results from the AMMA SOP0/DABEX and DODO field campaigns, Journal of Geophysical Research: Atmospheres, 113, n/a-n/a, 10.1029/2008JD009903, 2008.

Friese, C. A., van der Does, M., Merkel, U., Iversen, M. H., Fischer, G., and Stuut, J.-B. W.: Environmental factors controlling the seasonal variability in particle size distribution of modern Saharan dust deposited off Cape Blanc, Aeolian Research, 22, 165-179, http://dx.doi.org/10.1016/j.aeolia.2016.04.005, 2016.

Fütterer, D.: Sedimentation am NW-afrikanischen Kontinentalrand: Quantitative Zusammensetzung und Verteilung der Siltfraktion in den Oberflächensedimenten, Meteor-Forschungsergebnisse, C, 15-60, 1980.

Gac, J. Y., and Kane, A.: Le Fleuve Sénégal: I. Bilan hydrologique et flux continentaux de matières particulaires a l'embouchure, Sci. Géol. Bull., 39, 99-130, 1986.

García-Romero, E., Suárez, M., Santarén, J., and Alvarez, A.: Crystallochemical Characterization of the Palygorskite and Sepiolite from the Allou Kagne Deposit, Senegal, Clays and Clay Minerals, 55, 606-617, 10.1346/CCMN.2007.0550608, 2007.

1105 Gillies, J. A., Nickling, W. G., and McTainsh, G. H.: Dust concentrations and particle-size characteristics of an intense dust
1106 haze event: inland delta region, Mali, West Africa, Atmospheric Environment, 30, 1081-1090, 1996.

1107 Glaccum, R. A., and Prospero, J. M.: Saharan aerosols over the tropical North Atlantic - mineralogy, Marine Geology, 37, 295-
1108 321, 1980.

1109 Goossens, D., and Offer, Z. Y.: Wind tunnel and field calibration of six aeolian dust samplers, Atmospheric Environment, 34,
1110 1043-1057, 10.1016/s1352-2310(99)00376-3, 2000.

1111 Goossens, D.: Relationships between horizontal transport flux and vertical deposition flux during dry deposition of atmospheric
1112 dust particles, Journal of Geophysical Research: Earth Surface, 113, n/a-n/a, 10.1029/2007JF000775, 2008.

1113 Griffin, J. J., Windom, H., and Goldberg, E. D.: The distribution of clay minerals in the World Ocean, Deep Sea Research and
1114 Oceanographic Abstracts, 15, 433-459, http://dx.doi.org/10.1016/0011-7471(68)90051-X, 1968.

1115 Haywood, J., and Boucher, O.: Estimates of the direct and indirect radiative forcing due to tropospheric aerosols: A review,
1116 Rev Geophys, 38, 513-543, Doi 10.1029/1999rg000078, 2000.

1117 Holz, C., Stuut, J.-B. W., and Henrich, R.: Terrigenous sedimentation processes along the continental margin off NW-Africa:
1118 implications from grain-size analyses of surface sediments, Sedimentology, 51, 1145-1154, .1111/j.1365-3091.2004.00665.x,
1119 2004.

1120 Holz, C., Stuut, J.-B. W., Henrich, R., and Meggers, H.: Variability in terrigenous sedimentation processes off northwest Africa
1121 and its relation to climate changes: Inferences from grain-size distributions of a Holocene marine sediment record, Sedimentary
1122 Geology, 202, 499-508, 10.1016/j.sedgeo.2007.03.015, 2007.

1123 Iversen, M. H., Nowald, N., Ploug, H., Jackson, G. A., and Fischer, G.: High resolution profiles of vertical particulate organic
1124 matter export off Cape Blanc, Mauritania: Degradation processes and ballasting effects, Deep Sea Research Part I:
1125 Oceanographic Research Papers, 57, 771-784, DOI: 10.1016/j.dsr.2010.03.007, 2010.

1126 Iversen, M. H., and Ploug, H.: Ballast minerals and the sinking carbon flux in the ocean: carbon-specific respiration rates and
1127 sinking velocities of macroscopic organic aggregates (marine snow), Biogeosciences Discuss., 7, 3335-3364, 10.5194/bgd-7-
1128 3335-2010, 2010.

1129 Iversen, M. H., and Robert, M. L.: Ballasting effects of smectite on aggregate formation and export from a natural plankton
1130 community, Marine Chemistry, 175, 18-27, http://dx.doi.org/10.1016/j.marchem.2015.04.009, 2015.

1131 Jickells, T. D., An, Z. S., Andersen, K. K., Baker, A. R., Bergametti, G., Brooks, N., Cao, J. J., Boyd, P. W., Duce, R. A.,
1132 Hunter, K. A., Kawahata, H., Kubilay, N., laRoche, J., Liss, P. S., Mahowald, N., Prospero, J. M., Ridgwell, A. J., Tegen, I.,
1133 and Torres, R.: Global Iron Connections Between Desert Dust, Ocean Biogeochemistry, and Climate, Science, 308, 67-71,
1134 2005.

1135 Johnson, L. R.: Mineralogical dispersal patterns of North Atlantic deep-sea sediments with particular reference to eolian dusts,
1136 Marine Geology, 29, 335-345, http://dx.doi.org/10.1016/0025-3227(79)90115-4, 1979.

1137 Journet, E., Balkanski, Y., and Harrison, S. P.: A new data set of soil mineralogy for dust-cycle modeling, Atmos. Chem. Phys.,
1138 14, 3801-3816, 10.5194/acp-14-3801-2014, 2014.

1139 Kandler, K., Schütz, L., Deutscher, C., Ebert, M., Hofmann, H., Jäckel, S., Jaenicke, R., Knippertz, P., Lieke, K., Massling, A.,
1140 Petzold, A., Schladitz, A., Weinzierl, B., Wiedensohler, A., Zorn, S., and Weinbruch, S.: Size distribution, mass concentration,
1141 chemical and mineralogical composition and derived optical parameters of the boundary layer aerosol at Tinfou, Morocco,
1142 during SAMUM 2006, Tellus B, 61, 32-50, 10.1111/j.1600-0889.2008.00385.x, 2009.

1143 Khiri, F., Ezaidi, A., and Kabbachi, K.: Dust deposits in Souss-Massa basin, South-West of Morocco: granulometrical,
1144 mineralogical and geochemical characterisation, Journal of African Earth Sciences, 39, 459-464, 2004.

1145 Knippertz, P., and Todd, M. C.: Mineral dust aerosols over the Sahara: Meteorological controls on emission and transport and
1146 implications for modeling, Rev Geophys, 50, n/a-n/a, 10.1029/2011RG000362, 2012.

1147 Knippertz, P., and Stuut, J.-B. W.: Mineral dust a key player in the Earth system, Springer, Dordrecht, 2014.

1148 Koch, J., and Renno, N. O.: The role of convective plumes and vortices on the global aerosol budget, Geophysical Research
1149 Letters, 32, n/a-n/a, 10.1029/2005GL023420, 2005.

1150 Kogbe, C. A.: Geology of the upper cretaceous and tertiary sediments of the Nigerian sector of the Iullemeden Basin (West-
1151 Africa), Geol Rundsch, 62, 197-211, 10.1007/bf01826827, 1973.

1152 Koopmann, B.: Sedimentation von Saharastaub im subtropischen Nordatlantik während der letzten 25.000 Jahre, Meteor
1153 Forschungsergebnisse C, 35, 23-59, 1981.

1154 Korte, L. F., Brummer, G. J., van der Does, M., Guerreiro, C. V., Hennekam, R., van Hateren, J. A., Jong, D., Munday, C. I.,
1155 Schouten, S., and Stuut, J. B. W.: Downward particle fluxes of biogenic matter and Saharan dust across the equatorial North
1156 Atlantic., Atmos. Chem. Phys., 17,6023–6040, 10.5194/acp-17-6023-2017, 2017

1157 Lange, H.: Herkunft und Vertei-lung von Oberflachensedimenten des westafrikanischen Schelfs und Kontinentalhanges.‘,
1158 “Meteor” Forschungsergeb, 22, 61-84, 1975.

1159 Lange, H.: Distribution of Chlorite and Kaolinite in Eastern Atlantic Sediments Off North-Africa, Sedimentology, 29, 427-
1160 431, DOI 10.1111/j.1365-3091.1982.tb01805.x, 1982.

1161 Lau, K. M., and Kim, K. M.: Cooling of the Atlantic by Saharan dust, Geophys. Res. Lett., 34, 10.1029/2007GL031538, 2007.

1162 Martin, J. H.: Glacial-interglacial CO_2 change: the iron hypothesis, Paleoceanography, 5, 1-13, 1990.

1163 Martin, J. H., Gordon, R. M., and Fitzwater, S. E.: The case for iron, Limnology & Oceanography, 36, 1793-1802, 1991.

1164 McTainsh, G. H., Nickling, W. G., and Lynch, A. W.: Dust deposition and particle size in Mali, West Africa, Catena, 29, 307-
1165 322, 1997.

1166 Mendez, M. J., Funk, R., and Buschiazzo, D. E.: Field wind erosion measurements with Big Spring Number Eight (BSNE) and
1167 Modified Wilson and Cook (MWAC) samplers, Geomorphology, 129, 43-48, 10.1016/j.geomorph.2011.01.011, 2011.

1168 Meunier, T., Barton, E. D., Barreiro, B., and Torres, R.: Upwelling filaments off Cap Blanc: Interaction of the NW African
1169 upwelling current and the Cape Verde frontal zone eddy field?, Journal of Geophysical Research: Oceans, 117, n/a-n/a,
1170 10.1029/2012JC007905, 2012.

1171 Meyer, I., Davies, G. R., Vogt, C., Kuhlmann, H., and Stuut, J.-B. W.: Changing rainfall patterns in NW Africa since the
1172 Younger Dryas, Aeolian Research, 10, 111-123, http://dx.doi.org/10.1016/j.aeolia.2013.03.003, 2013.

1173 Mittelstaedt, E.: The ocean boundary along the northwest African coast: Circulation and oceanographic properties at the sea
1174 surface, Progress In Oceanography, 26, 307-355, 10.1016/0079-6611(91)90011-A, 1991.

1175 Moore, D. M., and Reynolds, R. C.: X-ray Diffraction and the Identification and Analysis of Clay Minerals, Oxford university
1176 press Oxford, 1989.

1177 Moreno, T., Querol, X., Castillo, S., Alastuey, A., Cuevas, E., Herrmann, L., Mounkaila, M., Elvira, J., and Gibbons, W.:
1178 Geochemical variations in aeolian mineral particles from the Sahara-Sahel Dust Corridor, Chemosphere, 65, 261-270, 2006.

1179 Mulitza, S., Heslop, D., Pittauerova, D., Fischer, H. W., Meyer, I., Stuut, J.-B., Zabel, M., Mollenhauer, G., Collins, J. A.,
1180 Kuhnert, H., and Schulz, M.: Increase in African dust flux at the onset of commercial agriculture in the Sahel region, Nature,
1181 466, 226-228, 10.1038/nature09213, 2010.

1182 National Geospatial-Intelligence Agency: North Atlantic, Baltic Sea, North Sea and Mediterranean Sea, 4 ed., Sailing directions
1183 (planning guide), ProStar Publications, 2006.

1184 Nicholson, S. E.: A revised picture of the structure of the "monsoon" and land ITCZ over West Africa, Climate Dynamics, 32,
1185 1155-1171, DOI 10.1007/s00382-008-0514-3, 2009.

1186 Nizou, J., Hanebuth, T. J. J., and Vogt, C.: Deciphering signals of late Holocene fluvial and aeolian supply from a shelf sediment
1187 depocentre off Senegal (north-west Africa), Journal of Quaternary Science, n/a-n/a, 10.1002/jqs.1467, 2011.

1188 Piqué, A.: Geology of northwest Africa, Gebrüder Borntraeger, 2001.

1189 Ploug, H., Iversen, M. H., and Fischer, G.: Ballast, sinking velocity, and apparent diffusivity within marine snow and
1190 zooplankton fecal pellets: Implications for substrate turnover by attached bacteria, Limnology and Oceanography, 53, 1878-
1191 1886, 2008a.

1192 Ploug, H., Iversen, M. H., Koski, M., and Buitenhuis, E. T.: Production, oxygen respiration rates, and sinking velocity of
1193 copepod fecal pellets: Direct measurements of ballasting by opal and calcite, Limnology and Oceanography, 53, 469-476, DOI
1194 10.4319/lo.2008.53.2.0469, 2008b.

1195 Proske, U., Hanebuth, T. J. J., Meggers, H., and Leroy, S. A. G.: Tidal flat sedimentation during the last millennium in the
1196 northern area of Tidra Island, Banc d'Arguin, Mauritania, Journal of African Earth Sciences, 50, 37-48,
1197 http://dx.doi.org/10.1016/j.jafrearsci.2007.09.002, 2008.

1198 Prospero, J. M., and Carlson, T. N.: Radon-222 in North Atlantic Trade Winds . Its Relationship to Dust Transport from Africa,
1199 Science, 167, 974-&, Doi 10.1126/Science.167.3920.974, 1970.

1200 Prospero, J. M., and Carlson, T. N.: Vertical and areal distribution of Saharan dust over the western equatorial north Atlantic
1201 Ocean, Journal of Geophysical Research, 77, 5255-5265, 10.1029/JC077i027p05255, 1972.

1202 Prospero, J. M., Ginoux, P., Torres, O., Nicholson, S. E., and Gill, T. E.: Environmental characterization of global sources of
1203 atmospheric soil dust identified with the Nimbus 7 total ozone mapping spectrometer (TOMS) absorbing aerosol product, Rev
1204 Geophys, 40, 1-31, 2002.

1205 Pye, K.: The nature, origin and accumulation of loess, Quaternary Science Reviews, 14, 653-667, 1995.

1206 Radczewski, O. E.: Eolian deposits in marine sediments, 1939.

Rateev, M. A., Gorbunova, Z. N., Lisitzyn, A. P., and Nosov, G. L.: THE DISTRIBUTION OF CLAY MINERALS IN THE OCEANS, Sedimentology, 13, 21-43, 10.1111/j.1365-3091.1969.tb01119.x, 1969.

Ratmeyer, V., Balzer, W., Bergametti, G., Chiapello, I., Fischer, G., and Wyputta, U.: Seasonal impact of mineral dust on deep-ocean particle flux in the eastern subtropical Atlantic Ocean, Marine Geology, 159, 241-252, 1999a.

Ratmeyer, V., Fischer, G., and Wefer, G.: Lithogenic particle fluxes and grain size distributions in the deep ocean off northwest Africa: Implications for seasonal changes of aeolian dust input and downward transport, Deep Sea Research Part I: Oceanographic Research Papers, 46, 1289-1337, 1999b.

Rea, D. K.: The paleoclimatic record provided by eolian deposition in the deep sea: the geologic history of wind, Rev Geophys, 32, 159-195, 1994.

Santamarina, J., and Cho, G.: Soil behaviour: The role of particle shape, Advances in geotechnical engineering: The skempton conference, 2004, 604-617,

Scheuvens, D., Schütz, L., Kandler, K., Ebert, M., and Weinbruch, S.: Bulk composition of northern African dust and its source sediments — A compilation, Earth-Science Reviews, 116, 170-194, http://dx.doi.org/10.1016/j.earscirev.2012.08.005, 2013.

Schlüter, T.: Geological atlas of Africa, Springer, 2008.

Schofield, D., Horstwood, M., Pitfield, P., Crowley, Q., Wilkinson, A., and Sidaty, H. C. O.: Timing and kinematics of Eburnean tectonics in the central Reguibat Shield, Mauritania, Journal of the Geological Society, 163, 549-560, 2006.

Schuster, M., Duringer, P., Ghienne, J.-F., Roquin, C., Sepulchre, P., Moussa, A., Lebatard, A.-E., Mackaye, H. T., Likius, A., Vignaud, P., and Brunet, M.: Chad Basin: Paleoenvironments of the Sahara since the Late Miocene, Comptes Rendus Geoscience, 341, 603-611, http://dx.doi.org/10.1016/j.crte.2009.04.001, 2009.

Schütz, L., and Sebert, M.: Mineral aerosols and source identification, Journal of Aerosol Science, 18, 1-10, http://dx.doi.org/10.1016/0021-8502(87)90002-4, 1987.

Selley, R. C.: Chapter 1 The sedimentary basins of northwest africa: stratigraphy and sedimentation, in: Sedimentary Basins of the World, edited by: Selley, R. C., Elsevier, 3-16, 1997a.

Selley, R. C.: Chapter 3 The sirte basin of libya, in: Sedimentary Basins of the World, edited by: Selley, R. C., Elsevier, 27-37, 1997b.

Selley, R. C.: Chapter 2 The basins of northwest africa: Structural evolution, in: Sedimentary Basins of the World, edited by: Selley, R. C., Elsevier, 17-26, 1997c.

Skonieczny, C., Bory, A., Bout-Roumazeilles, V., Abouchami, W., Galer, S. J. G., Crosta, X., Stuut, J. B., Meyer, I., Chiapello, I., Podvin, T., Chatenet, B., Diallo, A., and Ndiaye, T.: The 7-13 March 2006 major Saharan outbreak: Multiproxy characterization of mineral dust deposited on the West African margin, J. Geophys. Res., 116, D18210, 10.1029/2011jd016173, 2011.

Skonieczny, C., Bory, A., Bout-Roumazeilles, V., Abouchami, W., Galer, S. J. G., Crosta, X., Diallo, A., and Ndiaye, T.: A three-year time series of mineral dust deposits on the West African margin: Sedimentological and geochemical signatures and implications for interpretation of marine paleo-dust records, Earth and Planetary Science Letters, 364, 145-156, http://dx.doi.org/10.1016/j.epsl.2012.12.039, 2013.

1242 Stein, A. F., Draxler, R. R., Rolph, G. D., Stunder, B. J. B., Cohen, M. D., and Ngan, F.: NOAA's HYSPLIT Atmospheric
1243 Transport and Dispersion Modeling System, Bulletin of the American Meteorological Society, 96, 2059-2077, 10.1175/bams-
1244 d-14-00110.1, 2015.

1245 Stein, R.: Late neogene changes of paleoclimate and paleoproductivity off northwest africa (D.S.D.P. Site 397),
1246 Palaeogeography, Palaeoclimatology, Palaeoecology, 49, 47-59, http://dx.doi.org/10.1016/0031-0182(85)90004-5, 1985.

1247 Stuut, J.-B. W.: Late Quaternary Southwestern African terrestrial-climate signals in the marine record of Walvis Ridge, SE
1248 Atlantic Ocean, Faculty of Earth Sciences, Utrecht University, Utrecht, 128 pp., 2001.

1249 Stuut, J.-B. W., Zabel, M., Ratmeyer, V., Helmke, P., Schefuß, E., Lavik, G., and Schneider, R. R.: Provenance of present-day
1250 eolian dust collected off NW Africa, Journal of Geophysical Research, 110, 10.1029/2004JD005161, 2005.

1251 Stuut, J.-B. W., Smalley, I., and O'Hara-Dhand, K.: Aeolian dust in Europe: African sources and European deposits, Quaternary
1252 International, 198, 234-245, 10.1016/j.quaint.2008.10.007, 2009.

1253 Stuut, J.-B. W., Bakker, M., Friese, C., Koster, B., Visser, J.-D. d., and Witte, Y.: Cruise Report and preliminary results -
1254 DUSTTRAFFIC: Transatlantic fluxes of Saharan dust - Cruise No. 64PE392 - 19 – 27 August 2014 Las Palmas de Gran
1255 Canaria (Spain) – Mindelo, Sao Vicente (Cape Verdian Islands), 2015.

1256 Ternon, E., Guieu, C., Loÿe-Pilot, M. D., Leblond, N., Bosc, E., Gasser, B., Miquel, J. C., and Martín, J.: The impact of Saharan
1257 dust on the particulate export in the water column of the North Western Mediterranean Sea, Biogeosciences, 7, 809-826,
1258 10.5194/bg-7-809-2010, 2010.

1259 Tjallingii, R., Claussen, M., Stuut, J.-B. W., Fohlmeister, J., Jahn, A., Bickert, T., Lamy, F., and Rohl, U.: Coherent high- and
1260 low-latitude control of the northwest African hydrological balance, Nature Geoscience, 1, 670-675, 10.1038/ngeo289, 2008.

1261 Tsoar, H., and Pye, K.: Dust transport and the question of desert loess formation, Sedimentology, 34, 139-153, 1987.

1262 Tucker, M. E., and Tucker, M.: Techniques in sedimentology, 552.5. 08 TEC, 1988.

1263 Van Camp, L., Nykjaer, L., Mittelstaedt, E., and Schlittenhardt, P.: Upwelling and boundary circulation off Northwest Africa
1264 as depicted by infrared and visible satellite observations, Progress in Oceanography, 26, 357-402,
1265 http://dx.doi.org/10.1016/0079-6611(91)90012-B, 1991.

1266 Van der Does, M., Korte, L. F., Munday, C. I., Brummer, G. J. A., and Stuut, J. B. W.: Particle size traces modern Saharan dust
1267 transport and deposition across the equatorial North Atlantic, Atmos. Chem. Phys. Discuss., 2016, 1-27, 10.5194/acp-2016-
1268 344, 2016a.

1269 Van der Does, M., Korte, L. F., Munday, C. I., Brummer, G. J. A., and Stuut, J. B. W.: Particle size traces modern Saharan dust
1270 transport and deposition across the equatorial North Atlantic, Atmos. Chem. Phys., 16, 13697-13710, 10.5194/acp-16-13697-
1271 2016, 2016b.

1272 Verati, C., Bertrand, H., and Féraud, G.: The farthest record of the Central Atlantic Magmatic Province into West Africa craton:
1273 Precise 40Ar/39Ar dating and geochemistry of Taoudenni basin intrusives (northern Mali), Earth and Planetary Science Letters,
1274 235, 391-407, http://dx.doi.org/10.1016/j.epsl.2005.04.012, 2005.

1275 Villeneuve, M.: Paleozoic basins in West Africa and the Mauritanide thrust belt, Journal of African Earth Sciences, 43, 166-
1276 195, http://dx.doi.org/10.1016/j.jafrearsci.2005.07.012, 2005.

Vogt, C., Lauterjung, J., and Fischer, R. X.: Investigation of the Clay Fraction (< 2 μm) of the Clay Minerals Society Reference Clays, Clays and Clay Minerals, 50, 388-400, 2002.

Wilson, S., and Cooke, R.: Wind erosion, Soil erosion, 217251, 1980.

Wissmann, G.: Stratigraphy and structural features of the continental margin basin of Senegal and Mauritania, in: Geology of the Northwest African continental margin, Springer, 160-181, 1982.

Yoshioka, M., Mahowald, N. M., Conley, A. J., Collins, W. D., Fillmore, D. W., Zender, C. S., and Coleman, D. B.: Impact of Desert Dust Radiative Forcing on Sahel Precipitation: Relative Importance of Dust Compared to Sea Surface Temperature Variations, Vegetation Changes, and Greenhouse Gas Warming, Journal of Climate, 20, 1445-1467, doi:10.1175/JCLI4056.1, 2007.

Yu, H. B., Chin, M., Bian, H. S., Yuan, T. L., Prospero, J. M., Omar, A. H., Remer, L. A., Winker, D. M., Yang, Y. K., Zhang, Y., and Zhang, Z. B.: Quantification of trans-Atlantic dust transport from seven-year (2007-2013) record of CALIPSO lidar measurements, Remote Sens Environ, 159, 232-249, 10.1016/j.rse.2014.12.010, 2015.

Zobeck, T. M., Sterk, G., Funk, R., Rajot, J. L., Stout, J. E., and Van Pelt, R. S.: Measurement and data analysis methods for field-scale wind erosion studies and model validation, Earth Surface Processes and Landforms, 28, 1163-1188, 10.1002/esp.1033, 2003.